FAST FOURIER-LIKE MAPPED CHEBYSHEV SPECTRAL-GALERKIN METHODS FOR PDES WITH INTEGRAL FRACTIONAL LAPLACIAN IN UNBOUNDED DOMAINS[*]

CHANGTAO SHENG[†], JIE SHEN[‡], TAO TANG[§], LI-LIAN WANG[†], AND HUIFANG YUAN[¶]

Abstract. In this paper, we propose a fast spectral-Galerkin method for solving PDEs involving an integral fractional Laplacian in $\mathbb{R}^d$, which is built upon two essential components: (i) the Dunford–Taylor formulation of the fractional Laplacian; and (ii) Fourier-like biorthogonal mapped Chebyshev functions (MCFs) as basis functions. As a result, the fractional Laplacian can be fully diagonalized, and the complexity of solving an elliptic fractional PDE is quasi-optimal, i.e., $O((N\log_2 N)^d)$ with N being the number of modes in each spatial direction. Ample numerical tests for various decaying exact solutions show that the convergence of the fast solver perfectly matches the order of theoretical error estimates. With a suitable time discretization, the fast solver can be directly applied to a large class of nonlinear fractional PDEs. As an example, we solve the fractional nonlinear Schrödinger equation by using the fourth-order time-splitting method together with the proposed MCF–spectral-Galerkin method.

Key words. integral fractional Laplacian, Dunford–Taylor formula, mapped Chebyshev functions, biorthogonal basis functions, nonlocal/singular operators

AMS subject classifications. 65N35, 65M70, 41A05, 41A25

DOI. 10.1137/19M128377X

1. Introduction. Diffusion is the movement of a substance from an area of high concentration to an area of low concentration, which is a ubiquitous physical process in nature. The normal diffusion models rooted in Brownian motion have been well-studied for years. However, numerous experimental and scientific evidence has shown that many phenomena and complex systems involve anomalous diffusion, where the underlying stochastic processes are non-Brownian [41, 39, 40]. Notably, the fractional models have emerged as a powerful tool in modeling anomalous diffusion in diverse fields (see, e.g., [49, 28, 38, 18, 9, 13, 51, 15] and the references therein) over the past two decades. The nonlocal operators involved therein typically include the Riemann–Liouville, Caputo, and Riesz fractional integrals/derivatives, or the fractional Lapla-

[†]Division of Mathematical Sciences, School of Physical and Mathematical Sciences, Nanyang Technological University, 637371, Singapore (ctsheng@ntu.edu.sg, lilian@ntu.edu.sg).

[‡]Department of Mathematics, Purdue University, West Lafayette, IN 47907-1957 (shen7@purdue.edu).

[§]Division of Science and Technology, BNU-HKBU United International College, Zhuhai, Guangdong, China, and SUSTech International Center for Mathematics, Southern University of Science and Technology, Shenzhen, China (tangt@sustech.edu.cn).

[¶]Department of Mathematics, Southern University of Science and Technology, Shenzhen, 518055, China and School of Mathematics and Statistics, Wuhan University, Wuhan, 430072, China (yuanhf@sustech.edu.cn).

C. SHENG, J. SHEN, T. TANG, L.-L. WANG, AND H. YUAN

Downloaded 12/17/20 to 59.64.129.2. Redistribution subject to SIAM license or copyright; see https://epubs.siam.org/page/terms

cian. They share some common and interwoven difficulties, e.g., the nonlocal and singular behaviors, so they are much more challenging and difficult to deal with than the usual local operators. The recent works [34, 10] provide an up-to-date review in particular for numerical issues with several versions of the fractional Laplacian. The interested readers are also referred to [50, 22, 19] for nonlocal and fractional modeling in many other applications.

A large volume of literature is available for numerical solutions of one-dimensional spatial and temporal fractional differential equations, which particularly include the finite difference methods/finite element methods (see, e.g., [20, 23, 27, 31, 32, 57] and many references therein), and spectral methods (see, e.g., [16, 29, 36]). In this work, we are mainly interested in the integral fractional Laplaican in multiple dimensions, which is deemed as one of the most challenging nonlocal operators for both computation and analysis. It is known that for $s \in (0,1)$, the fractional Laplacian of $u \in \mathscr{S}(\mathbb{R}^d)$ (the functions of the Schwartz class) is defined by the Fourier transform

$$(1.1) \qquad (-\Delta)^s u(x) := \mathscr{F}^{-1}\big[|\xi|^{2s}\mathscr{F}[u](\xi)\big](x) \quad \forall\, x \in \mathbb{R}^d.$$

Equivalently, it can be defined by the pointwise formula (cf. [42, Prop. 3.3])

$$(1.2) \qquad (-\Delta)^s u(x) = C_{d,s}\, \mathrm{p.v.}\!\int_{\mathbb{R}^d} \frac{u(x) - u(y)}{|x - y|^{d+2s}}\, \mathrm{d}y, \quad x \in \mathbb{R}^d,$$

where "p.v." stands for the principle value and the normalization constant

$$(1.3) \qquad C_{d,s} := \bigg(\int_{\mathbb{R}^d} \frac{1 - \cos \xi_1}{|\xi|^{d+2s}}\, \mathrm{d}\xi\bigg)^{-1} = \frac{2^{2s} s\, \Gamma(s + d/2)}{\pi^{d/2}\Gamma(1 - s)}.$$

As a result, to evaluate the fractional diffusion of u at a spatial point, information involving all spatial points is needed. If u is defined on a bounded domain Ω, we first extend it to zero outside Ω, and then use the above definition.

As many physically motivated fractional diffusion models are naturally set in unbounded domains, the development of effective solution methods has attracted much recent attention. In general, the existing approaches can be classified into the following two categories.

- This first is to approximate the solution by the orthogonal basis functions, and fully use the analytic properties of the fractional Laplacian performing on the basis (see, e.g., [17, 37, 55, 54]). Based on some analytic fractional calculus formulas of generalized Laguerre functions, Chen, Shen, and Wang [17] developed an efficient spectral method for the one-dimensional fractional Laplacian on the whole line. Using the property that the Hermite functions are invariant under the Fourier transform, Mao and Shen [37] proposed the Hermite spectral-Galerkin method in the transformed domain based on the Fourier definition (1.1). Tang, Yuan, and Zhou [55] explicitly evaluated the Hermite fractional differentiation matrices and implemented the spectral-collocation methods based on some elegant analytic tools. The idea was extended to the rational approximation in [54]. It is noteworthy that due to the singular and nonseparable factor $|\xi|^{2s}$ in (1.1), these methods become complicated even for $d = 2$, and computationally prohibitive for $d \geq 3$.
- The second is to use suitable equivalent formulations of the fractional Laplacian to alleviate its notorious numerical difficulties. In Caffarelli and Silvestre [14], the d-dimensional fractional Laplacian is extended to a $d+1$ dimensional

Copyright © by SIAM. Unauthorized reproduction of this article is prohibited.

elliptic operator with degenerating/singular coefficients in the additional dimension. This groundbreaking extension, together with the follow-up works for the fractional Laplacian in bounded domains, provides a viable alternative for its mathematical and numerical treatment (see, e.g., [43, 44, 5] for finite element methods). On the other hand, the variational form corresponding to the fractional Laplacian can be formulated as the Dunford–Taylor formula (cf. [11, Thm. 4.1]): for any $u, v \in H^s(\mathbb{R}^d)$ with $s \in (0,1)$,

$$
(1.4) \quad \begin{aligned}
&\left((-\Delta)^{\frac{s}{2}} u, (-\Delta)^{\frac{s}{2}} v\right)_{L^2(\mathbb{R}^d)} \\
&\quad = C_s \int_0^\infty t^{1-2s} \int_{\mathbb{R}^d} \left((-\Delta)(\mathbb{I} - t^2 \Delta)^{-1} u\right)(x)\, v(x) \, \mathrm{d}x \, \mathrm{d}t,
\end{aligned}
$$

where $\mathbb{I}$ is the identity operator and $C_s = 2 \sin(\pi s)/\pi$. In particular, for the fractional Laplacian in a bounded domain $\Omega \subseteq \mathbb{R}^d$, we have

$$
(1.5) \quad \begin{aligned}
&\left((-\Delta)^{\frac{s}{2}} \tilde{u}, (-\Delta)^{\frac{s}{2}} \tilde{v}\right)_{L^2(\Omega)} \\
&\quad = C_s \int_0^\infty t^{1-2s} \int_\Omega \left((-\Delta)(\mathbb{I} - t^2 \Delta)^{-1} \tilde{u}\right)(x)\, v(x) \, \mathrm{d}x \, \mathrm{d}t,
\end{aligned}
$$

where $\tilde{u}$ denotes the zero extension of u. Very recently, the finite element method with sinc quadrature (in t), was implemented and analyzed in [11, 12] based on (1.5). For each quadrature node t_j, one solves the elliptic problem

$$
(1.6) \qquad -t_j^2 \Delta w_j + w_j = \tilde{u} \quad \text{in } \mathbb{R}^d, \quad \text{i.e., } w_j = (\mathbb{I} - t_j^2 \Delta)^{-1} \tilde{u}(x),
$$

where the unbounded domain has to be truncated, and the size of the domain depends on t_j. In fact, many sinc quadrature points should be used to resolve the singularity near $t = 0$, but the problem (1.6) becomes stiff and sharp boundary layers at $\partial\Omega$ can occur.

We also remark that direct discretization of the integral fractional Laplacian on bounded domains based on the definition (1.2), was discussed in some recent works (see, e.g., [30, 24] for finite difference methods and [2, 1, 4, 5, 21] for finite element methods).

In this paper, we develop a fast spectral-Galerkin method for PDEs involving an integral fractional Laplacian in $\mathbb{R}^d$. Consider, for example, the model equation

$$
(1.7) \qquad (-\Delta)^s u(x) + \gamma u(x) = f(x) \quad \text{in } \mathbb{R}^d; \quad u(x) \to 0 \quad \text{as } |x| \to \infty,
$$

where $s \in (0,1)$ and $\gamma > 0$. The efficient spectral algorithm is built upon two essential components: (i) the Dunford–Taylor formulation (1.4) for the fractional Laplacian; and (ii) the approximation of the solution by the tensorial Fourier-like biorthogonal mapped Chebyshev functions. As a result, the complexity of solving (1.7) is $O((N \log_2 N)^d)$, where N is the degree of freedom along each spatial dimension. The integration in t (in (1.4)) can be evaluated exactly by using such a formulation and basis, so the main computational cost is from the mapped Chebyshev function (MCF) expansions with FFT. In fact, the framework is also applicable to Hermite functions, but Hermite approximation is less compelling for at least two reasons: (i) the lack of FFT; and (ii) slow decay of the solution or the source term. As opposed to the usual Laplacian, the fractional Laplacian of a function with typical exponential or algebraic decay will decay algebraically at a much slower rate (see Propositions 4.2–4.3 of this paper). Thus, the MCF approximation is more preferable. Indeed, ample numerical

results show that the fast solver for (1.7) has a convergence behavior in agreement with the theoretical estimate for various decaying exact solutions being tested.

The rest of this paper is organized as follows. In section 2, we first introduce the MCFs and generate the Fourier-like biorthogonal MCFs in one dimension. In section 3, we describe the fast MCF–spectral-Galerkin method built upon the Dunford–Taylor formulation of the fractional Laplacian. We conduct the error estimates and provide ample numerical results to show the convergence order of the solver is in agreement with the theoretical prediction in section 4. In the final section, we apply the solver to spatial discretization of the fractional nonlinear Schrödinger equation, and also conclude the paper with some final remarks.

2. Fourier-like MCFs. In this section, we introduce the MCFs, from which we construct the Fourier-like biorthogonal MCFs as one of the important tools for the efficient spectral algorithms to be designed in the forthcoming section.

2.1. Mapped Chebyshev functions. Let $T_n(y) = \cos(n \arccos(y))$, $y \in \Lambda := (-1, 1)$ be the Chebyshev polynomial of degree n. The Chebyshev polynomials satisfy the three-term recurrence relation

$$(2.1) \qquad T_{n+1}(y) = 2y T_n(y) - T_{n-1}(y), \quad n \geq 1,$$

with $T_0(y) = 1$ and $T_1(y) = y$. They form a complete orthogonal system in $L_\omega^2(\Lambda)$, namely,

$$(2.2) \qquad \int_\Lambda T_n(y) T_m(y) \omega(y) \, dy = \frac{\pi c_n}{2} \delta_{nm} \quad \text{with} \quad \omega(y) = (1 - y^2)^{-\frac{1}{2}}$$

where δ_{nm} is the Kronecker symbol, and $c_0 = 2$ and $c_n = 1$ for $n \geq 1$. Recall the recurrence formulas (cf. [52])

$$(2.3) \quad y T_n(y) = (T_{n+1}(y) + T_{n-1}(y))/2, \quad (1 - y^2) T_n'(y) = \frac{n}{2}(T_{n-1}(y) - T_{n+1}(y)).$$

We now define the MCFs as in [26, 45, 48].

DEFINITION 2.1. *Introduce the one-to-one algebraic mapping*

$$(2.4) \qquad x = \frac{y}{\sqrt{1 - y^2}}, \quad y = \frac{x}{\sqrt{1 + x^2}}, \quad x \in \mathbb{R}, \ y \in \Lambda,$$

and define the MCFs as

$$(2.5) \qquad \mathbb{T}_n(x) = \frac{1}{\sqrt{c_n \pi / 2}} \sqrt{1 - y^2} \, T_n(y) = \frac{1}{\sqrt{c_n \pi / 2}} \frac{1}{\sqrt{1 + x^2}} T_n\left(\frac{x}{\sqrt{1 + x^2}}\right)$$

for $x \in \mathbb{R}$ and integer $n \geq 0$.

Remark 2.1. As with the Hermite approximation (cf. [53, 45]), one can incorporate a scaling factor $\nu > 0$ to improve the performance of the MCF approximation. More precisely, using the mapping

$$x = \frac{\nu y}{\sqrt{1 - y^2}}, \quad y = \frac{x}{\sqrt{\nu^2 + x^2}}, \quad x \in \mathbb{R}, \ y \in \Lambda, \ \nu > 0,$$

the scaled MCFs can be defined as

$$\mathbb{T}_n^\nu(x) := \frac{1}{\sqrt{c_n \pi / 2}} \frac{\nu^{1/2}}{\sqrt{\nu^2 + x^2}} T_n\left(\frac{x}{\sqrt{\nu^2 + x^2}}\right) = \frac{1}{\sqrt{\nu}} \mathbb{T}_n\left(\frac{x}{\nu}\right).$$

Following [46, 47], we examine the collocation/quadrature points mapped from the Chebyshev–Gauss points $\{y_j = -\cos(\frac{(2j-1)\pi}{2N})\}_{j=1}^N$. Note that the mapped points are distributed in $[x_1, x_N]$ with

$$x_N = -x_1 = \nu \cot \frac{\pi}{2N} \approx \frac{2\nu}{\pi} N,$$

and by the mean value theorem, the stretching of the Chebyshev–Gauss points obeys the rule

$$x_{j+1} - x_j = \frac{\nu}{(1 - \xi_j^2)^{5/2}} (y_{j+1} - y_j), \ \ \exists \xi_j \in (y_j, y_{j+1}).$$

It is seen that the scaling factor offers a flexibility to tune the distribution of points so that most of then can be distributed in an interval containing the portion of the solution of physical interest (cf. [53]). In principle, we can choose ν adaptively depending on N or time for time-dependent problems (cf. [35]). We remark it is straightforward to extend the properties and algorithms from the usual MCFs to the scaled MCFs with a constant scaling factor. For clarity of presentation, we shall not carry the scaling parameter in the algorithm descriptions and error analysis, but use it in the numerical experiments.

We have the following important properties of the MCFs, which can be shown readily by using Definition 2.1 and the properties of Chebyshev polynomials in (2.1)–(2.3) (also see [48, Prop. 2.4]).

PROPOSITION 2.1. *The MCFs are orthonormal in $L^2(\mathbb{R})$, and we have*

$$S_{mn} = S_{nm} = \int_{\mathbb{R}} \mathbb{T}_n'(x)\, \mathbb{T}_m'(x)\, \mathrm{d}x$$

$$= \begin{cases} \frac{1}{c_n}\Big(\frac{(4c_{n-1} - c_{n-2})(n-1)^2}{16} + \frac{(4c_{n+1} - c_{n+2})(n+1)^2}{16} - \frac{c_n}{4}\Big) & \text{if } m = n, \\ \frac{1}{\sqrt{c_n c_{n+2}}}\Big(\frac{(c_n - c_{n+2})(n+1)}{8} - \frac{c_{n+1}(n+1)^2}{4}\Big) & \text{if } m = n+2, \\ \frac{1}{\sqrt{c_n c_{n+4}}}\Big(\frac{c_{n+2}(n+1)(n+3)}{16}\Big) & \text{if } m = n+4, \\ 0 & \text{otherwise.} \end{cases}$$

2.2. Fourier-like biorthogonal MCFs in one dimension. Let $\mathbb{P}_N$ be the set of all polynomials of degree at most N, and define the finite-dimensional space

$$(2.6) \qquad \mathbb{V}_N := \big\{\phi : \phi(x) = g(x)\varphi(x) \ \forall\, \varphi \in \mathbb{P}_N\big\},$$

where x, y are associated with the mapping (2.4) and

$$(2.7) \qquad g(x) := \sqrt{\omega(y)\frac{\mathrm{d}y}{\mathrm{d}x}} = \frac{1}{\sqrt{1 + x^2}} = \sqrt{1 - y^2} := G(y).$$

Note that we have

$$(2.8) \qquad \mathbb{V}_N := \mathrm{span}\big\{\mathbb{T}_n(x) : 0 \le n \le N\big\}.$$

Following the spirit of [47], we next introduce a Fourier-like basis of $\mathbb{V}_N$, which is orthogonal in both L^2- and H^1-inner-products. For this purpose, let $\boldsymbol{S}$ be a square matrix of order $N+1$ with entries given in Proposition 2.1, and let $\boldsymbol{I}$ be the identity matrix

of the same size. Observe that $\boldsymbol{S}$ is a symmetric sparse nine-diagonal matrix with five nonzero diagonals. Moreover, we can show that $\boldsymbol{S}$ is a positive definite matrix. Indeed, for any nonzero vector $\hat{\boldsymbol{v}} = (\hat{v}_0, \ldots, \hat{v}_N)^t$, we define $v_N(x) = \sum_{n=0}^{N} \hat{v}_n \mathbb{T}_n(x) (\in \mathbb{V}_N)$. One readily verifies that

$$\hat{\boldsymbol{v}}^t \boldsymbol{S} \hat{\boldsymbol{v}} = \sum_{m,n=0}^{N} \hat{v}_m \hat{v}_n \int_{\mathbb{R}} \mathbb{T}'_n(x)\,\mathbb{T}'_m(x)\,\mathrm{d}x = \int_{\mathbb{R}} (v'_N(x))^2 \,\mathrm{d}x > 0,$$

which is strictly positive as the space $\mathbb{V}_N$ by definition does not contain a nonzero constant. Thus, $\boldsymbol{S}$ is a symmetric positive definite matrix, whose eigenvalues are all real and positive, and the eigenvectors are orthonormal. To this end, let $\boldsymbol{E} = (e_{jk})_{j,k=0,\ldots,N}$ be the matrix formed by the orthonormal eigenvectors of $\boldsymbol{S}$, and $\boldsymbol{\Sigma} = \mathrm{diag}\{\lambda_k\}$ be the diagonal matrix of the corresponding eigenvalues. Thus, we have

(2.9) $$\boldsymbol{SE} = \boldsymbol{E}\,\boldsymbol{\Sigma}, \quad \boldsymbol{E}^t \boldsymbol{E} = \boldsymbol{I}.$$

We remark that with an even and odd separation, we can work with two symmetric positive definite seven-diagonal submatrices to compute the eigenvalues and eigenvectors of $\boldsymbol{S}$, which should be more stable for large N.

LEMMA 2.1. *Let $\boldsymbol{E} = (\boldsymbol{e}_0, \boldsymbol{e}_1, \ldots, \boldsymbol{e}_N)$ be the matrix of the eigenvectors of $\boldsymbol{S}$, i.e., $\boldsymbol{S}\boldsymbol{e}_p = \lambda_p \boldsymbol{e}_p$ for $0 \le p \le N$. Define*

(2.10) $$\widehat{\mathbb{T}}_p(x) := \sum_{j=0}^{N} e_{jp} \mathbb{T}_j(x), \quad \boldsymbol{e}_p = (e_{0p}, e_{1p}, \ldots, e_{Np})^t, \quad 0 \le p \le N.$$

Then $\{\widehat{\mathbb{T}}_p\}_{p=0}^{N}$ form an equivalent basis of $\mathbb{V}_N$, and they are biorthogonal in the sense that

(2.11) $$(\widehat{\mathbb{T}}_p, \widehat{\mathbb{T}}_q)_{L^2(\mathbb{R})} = \delta_{pq}, \quad \left(\widehat{\mathbb{T}}'_p, \widehat{\mathbb{T}}'_q\right)_{L^2(\mathbb{R})} = \lambda_p \delta_{pq}, \quad 0 \le p, q \le N.$$

Proof. In view of the definition (2.10), we infer from the orthogonality of MCFs and (2.9) that

$$(\widehat{\mathbb{T}}_p, \widehat{\mathbb{T}}_q)_{L^2(\mathbb{R})} = \sum_{j=0}^{N} \sum_{k=0}^{N} e_{kp} e_{jq} (\mathbb{T}_k, \mathbb{T}_j)_{L^2(\mathbb{R})}$$
$$= \sum_{j=0}^{N} \sum_{k=0}^{N} e_{jq} \delta_{jk} e_{kp} = \sum_{k=0}^{N} e_{kq} e_{kp} = \boldsymbol{e}_q^t \boldsymbol{e}_p = \delta_{pq}.$$

Similarly, we can show that

$$\left(\widehat{\mathbb{T}}'_p, \widehat{\mathbb{T}}'_q\right)_{L^2(\mathbb{R})} = \sum_{j=0}^{N} \sum_{k=0}^{N} e_{kp} e_{jq} (\mathbb{T}'_k, \mathbb{T}'_j)_{L^2(\mathbb{R})}$$
$$= \sum_{j=0}^{N} \sum_{k=0}^{N} e_{jq} S_{jk} e_{kp} = (\boldsymbol{E}^t \boldsymbol{S} \boldsymbol{E})_{pq} = (\boldsymbol{\Sigma})_{pq} = \lambda_p \delta_{pq}.$$

This ends the proof.   □

3. MCF–spectral-Galerkin method based on the Dunford–Taylor formulation. In this section, we describe the fast MCF–spectral-Galerkin algorithm for a model elliptic problem with integral fractional Laplacian. We then apply the solver for spatial discretization of some nonlinear fractional PDEs in the next section.

3.1. Some notation. Denote by $\mathscr{S}(\mathbb{R}^d)$ the functions of the Schwartz class, and let $\mathscr{S}'(\mathbb{R}^d)$ be the topological dual of $\mathscr{S}(\mathbb{R}^d)$. For any $u \in \mathscr{S}(\mathbb{R}^d)$, its Fourier transform is given by

$$\mathscr{F}[u](\xi) = \frac{1}{(2\pi)^{\frac{d}{2}}} \int_{\mathbb{R}^d} u(x) e^{-\mathrm{i}\xi \cdot x} \mathrm{d}x \quad \forall \xi \in \mathbb{R}^d.$$

For real $s \geq 0$, we define the fractional Sobolev space (cf. [42, p. 530]):

$$(3.1) \quad H^s(\mathbb{R}^d) = \Big\{ u \in L^2(\mathbb{R}^d) : \|u\|_{H^s(\mathbb{R}^d)}^2 = \int_{\mathbb{R}^d} (1 + |\xi|^{2s}) \big|\mathscr{F}[u](\xi)\big|^2 \mathrm{d}\xi < +\infty \Big\},$$

and an analogous definition for the case $s < 0$ is to set

$$(3.2) \quad H^s(\mathbb{R}^d) = \Big\{ u \in \mathscr{S}'(\mathbb{R}^d) : \|u\|_{H^s(\mathbb{R}^d)}^2 = \int_{\mathbb{R}^d} (1 + |\xi|^2)^s \big|\mathscr{F}[u](\xi)\big|^2 \mathrm{d}\xi < +\infty \Big\},$$

although in this case the space $H^s(\mathbb{R}^d)$ is not a subset of $L^2(\mathbb{R}^d)$.

According to [42, Prop. 3.4], we know that for $s \in (0, 1)$, the space $H^s(\mathbb{R}^d)$ can also be characterized by the fractional Laplacian defined in (1.2), equipped with the norm

$$\|u\|_{H^s(\mathbb{R}^d)} = \big(\|u\|_{L^2(\mathbb{R}^d)}^2 + [u]_{H^s(\mathbb{R}^d)}^2 \big)^{\frac{1}{2}},$$

where $[u]_{H^s(\mathbb{R}^d)}$ is the so-called Gagliardo (semi)norm of u, given by

$$(3.3) \quad [u]_{H^s(\mathbb{R}^d)} = \Big(\int_{\mathbb{R}^d} \int_{\mathbb{R}^d} \frac{|u(x) - u(y)|^2}{|x - y|^{d+2s}} \mathrm{d}x\mathrm{d}y \Big)^{\frac{1}{2}}.$$

Indeed, by [42, Prop. 3.6], we have that for $s \in (0, 1)$,

$$(3.4) \quad [u]_{H^s(\mathbb{R}^d)}^2 = 2C_{d,s}^{-1} \|(-\Delta)^{s/2} u\|_{L^2(\mathbb{R}^d)}^2.$$

We have the following important space interpolation property (cf. [3, Chap. 1]), which will be used for the error analysis later on.

LEMMA 3.1. *For real $r_0, r_1 \geq 0$, let $r = (1 - \theta)r_0 + \theta r_1$ with $\theta \in [0, 1]$. Then for any $u \in H^{r_0}(\mathbb{R}^d) \cap H^{r_1}(\mathbb{R}^d)$, we have*

$$(3.5) \quad \|u\|_{H^r(\mathbb{R}^d)} \leq \|u\|_{H^{r_0}(\mathbb{R}^d)}^{1-\theta} \|u\|_{H^{r_1}(\mathbb{R}^d)}^{\theta}.$$

In particular, for $s \in [0, 1]$, we have

$$(3.6) \quad \|u\|_{H^s(\mathbb{R}^d)} \leq \|u\|_{L^2(\mathbb{R}^d)}^{1-s} \|u\|_{H^1(\mathbb{R}^d)}^s.$$

3.2. Dunford–Taylor formulation of the fractional Laplacian. To fix the idea, we consider

$$(3.7) \quad (-\Delta)^s u(x) + \gamma u(x) = f(x) \quad \text{in } \mathbb{R}^d, \quad u(x) = 0 \quad \text{as } |x| \to \infty,$$

where $s \in (0, 1), \gamma > 0$, and $f \in H^{-s}(\mathbb{R}^d)$.

A weak form for (3.7) is to find $u \in H^s(\mathbb{R}^d)$ such that

(3.8)
$$\mathcal{B}(u,v) = \big((-\Delta)^{s/2}u, (-\Delta)^{s/2}v\big)_{L^2(\mathbb{R}^d)} + \gamma(u,v)_{L^2(\mathbb{R}^d)}$$
$$= [u,v]_{H^s(\mathbb{R}^d)} + \gamma(u,v)_{L^2(\mathbb{R}^d)} = (f,v)_{L^2(\mathbb{R}^d)} \quad \forall v \in H^s(\mathbb{R}^d),$$

where $[u,v]_{H^s(\mathbb{R}^d)}$ induces the Gagliardo (semi)norm in (3.3). Here, we understand the inner product at the right-hand side as the duality pairing between $H^{-s}(\mathbb{R}^d)$ and $H^s(\mathbb{R}^d)$.

By the definitions (1.1) and (3.1), we immediately obtain the continuity and coercivity of the bilinear form $a(\cdot,\cdot)$, that is, for any $u,v \in H^s(\mathbb{R}^d)$,

(3.9)
$$|\mathcal{B}(u,v)| \lesssim \|u\|_{H^s(\mathbb{R}^d)}\|v\|_{H^s(\mathbb{R}^d)}, \quad |\mathcal{B}(u,u)| \gtrsim \|u\|^2_{H^s(\mathbb{R}^d)}.$$

Then, we derive from the Lax–Milgram lemma (cf. [6]) that the problem (3.8) admits a unique solution satisfying

$$\|u\|_{H^s(\mathbb{R}^d)} \lesssim \|f\|_{H^{-s}(\mathbb{R}^d)}.$$

In view of the definitions in (1.1)–(1.2), we have the equivalent forms of $[u,v]_{H^s(\mathbb{R}^d)}$ as follows:

(3.10)
$$[u,v]_{H^s(\mathbb{R}^d)} = \int_{\mathbb{R}^d}\int_{\mathbb{R}^d} \frac{(u(x)-u(y))(v(x)-v(y))}{|x-y|^{d+2s}}\mathrm{d}x\mathrm{d}y$$

(3.11)
$$= \int_{\mathbb{R}^d} |\xi|^{2s}\mathscr{F}[u](\xi)\overline{\mathscr{F}[v](\xi)}\,\mathrm{d}\xi.$$

It is noteworthy that the direct implementation of a numerical scheme based on (3.10) (i.e., in physical space) is very difficult. Most of the existing works (see, e.g., [37, 55, 54]) are therefore mainly based on (3.11) (i.e., in the frequency space). The Hermite function approaches can take advantage that the Fourier transforms of Hermite functions are explicitly known. However, in multiple dimensions, the non-separable/singular factor $|\xi|^{2s} = (\xi_1^2 + \cdots + \xi_d^2)^s$ makes the tensorial approach computationally prohibitive. On the other hand, the fractional Laplacian operator may become rather complicated when a coordinate transform is applied, so the mapped Chebyshev approximation cannot be applied in either of the above formulations.

In what follows, we resort to an alternative formulation of the fractional Laplacian that can overcome these numerical difficulties. According to [11, Thm. 4.1], we have the following Dunford–Taylor formulation of the integral fractional Laplacian.

LEMMA 3.2. *For any $u,v \in H^s(\mathbb{R}^d)$ with $s \in (0,1)$, we have*

(3.12)
$$\big((-\Delta)^{\frac{s}{2}}u, (-\Delta)^{\frac{s}{2}}v\big)_{L^2(\mathbb{R}^d)}$$
$$= C_s \int_0^\infty t^{1-2s} \int_{\mathbb{R}^d} \big((-\Delta)(\mathbb{I}-t^2\Delta)^{-1}u\big)(x)\,v(x)\,\mathrm{d}x\,\mathrm{d}t,$$

where $\mathbb{I}$ is the identity operator and

(3.13)
$$C_s = \frac{2\sin(\pi s)}{\pi}.$$

Let us denote $w = w(u,t) := (\mathbb{I}-t^2\Delta)^{-1}u(x)$. Then there holds

(3.14) $-t^2\Delta w + w = u$ in $\mathbb{R}^d$, so $(-\Delta)(\mathbb{I}-t^2\Delta)^{-1}u = -\Delta w = t^{-2}(u-w)$.

As a result, we can rewrite the weak form (3.8) as finding $u \in H^s(\mathbb{R}^d)$ such that

$$
(3.15) \quad
\begin{aligned}
\mathcal{B}(u, v) &= C_s \int_0^\infty t^{-1-2s}(u - w, v)_{L^2(\mathbb{R}^d)}\, \mathrm{d}t + \gamma\,(u, v)_{L^2(\mathbb{R}^d)} \\
&= (f, v)_{L^2(\mathbb{R}^d)} \quad \forall v \in H^s(\mathbb{R}^d),
\end{aligned}
$$

where $w = w(u, t)$ solves

$$
(3.16) \quad t^2 (\nabla w, \nabla \psi)_{L^2(\mathbb{R}^d)} + (w, \psi)_{L^2(\mathbb{R}^d)} = (u, \psi)_{L^2(\mathbb{R}^d)} \quad \forall \psi \in H^1(\mathbb{R}^d).
$$

It is evident that the well-posedness of (3.15)–(3.16) follows from its equivalence to (3.8).

3.3. The MCF–spectral-Galerkin scheme and its implementation. Define

$$
(3.17) \quad \mathbb{V}_N^d = \mathbb{V}_N \otimes \cdots \otimes \mathbb{V}_N,
$$

which is the tensor product of d copies of $\mathbb{V}_N$ defined in (2.6). Here, $\mathbb{V}_N^1 = \mathbb{V}_N$, and denote $I_N^d : C(\mathbb{R}^d) \to \mathbb{V}_N^d$ the tensorial mapped Chebyshev interpolation operator. The MCF–spectral-Galerkin approximation to (3.15)–(3.16) is to find $u_N \in \mathbb{V}_N^d$ such that

$$
(3.18) \quad
\begin{aligned}
\mathcal{B}_N(u_N, v_N) &= C_s \int_0^\infty t^{-1-2s}(u_N - w_N, v_N)_{L^2(\mathbb{R}^d)}\, \mathrm{d}t + \gamma\,(u_N, v_N)_{L^2(\mathbb{R}^d)} \\
&= (I_N^d f, v_N)_{L^2(\mathbb{R}^d)} \quad \forall v_N \in \mathbb{V}_N^d,
\end{aligned}
$$

where we find $w_N := w_N(u_N, t) \in \mathbb{V}_N^d$ such that for any $t > 0$,

$$
(3.19) \quad t^2 (\nabla w_N, \nabla \psi)_{L^2(\mathbb{R}^d)} + (w_N, \psi)_{L^2(\mathbb{R}^d)} = (u_N, \psi)_{L^2(\mathbb{R}^d)} \quad \forall \psi \in \mathbb{V}_N^d.
$$

Define the d-dimensional tensorial Fourier-like basis and denote the vector of the corresponding eigenvalues in (2.9) by

$$
(3.20) \quad \widehat{\mathbb{T}}_n(x) = \prod_{j=1}^d \widehat{\mathbb{T}}_{n_j}(x_j) \quad x \in \mathbb{R}^d, \quad \lambda_n = (\lambda_{n_1}, \ldots, \lambda_{n_d})^t.
$$

Accordingly, we have

$$
(3.21) \quad \mathbb{V}_N^d = \mathrm{span}\big\{\widehat{\mathbb{T}}_n(x),\ n \in \Upsilon_N\big\},
$$

where the index set

$$
(3.22) \quad \Upsilon_N := \big\{ n = (n_1, \ldots, n_d) \,:\, 0 \le n_j \le N,\ 1 \le j \le d \big\}.
$$

As an extension of (2.11), we have the following attractive property of the tensorial Fourier-like MCFs.

THEOREM 3.1. *For the tensorial Fourier-like MCFs, we have*

$$
(3.23) \quad (\widehat{\mathbb{T}}_p, \widehat{\mathbb{T}}_q)_{L^2(\mathbb{R}^d)} = \delta_{pq}, \quad \big(\nabla \widehat{\mathbb{T}}_p, \nabla \widehat{\mathbb{T}}_q\big)_{L^2(\mathbb{R}^d)} = |\lambda_p|_1\, \delta_{pq},
$$

where $p, q \in \Upsilon_N$ and

$$
(3.24) \quad \delta_{pq} = \prod_{j=0}^d \delta_{p_j q_j}, \quad |\lambda_p|_1 = \lambda_{p_1} + \cdots + \lambda_{p_d}.
$$

Proof. One verifies by using the orthogonality (2.11) and the definition (3.20) that

$$(\widehat{\mathbb{T}}_p, \widehat{\mathbb{T}}_q)_{L^2(\mathbb{R}^d)} = (\widehat{\mathbb{T}}_{p_1}, \widehat{\mathbb{T}}_{q_1})_{L^2(\mathbb{R})} \cdots (\widehat{\mathbb{T}}_{p_d}, \widehat{\mathbb{T}}_{q_d})_{L^2(\mathbb{R})} = \delta_{p_1 q_1} \cdots \delta_{p_d q_d} = \delta_{pq},$$

and

$$\begin{aligned}
(\nabla\widehat{\mathbb{T}}_p, \nabla\widehat{\mathbb{T}}_q)_{L^2(\mathbb{R}^d)} &= \big\{ (\widehat{\mathbb{T}}'_{p_1}, \widehat{\mathbb{T}}'_{q_1})_{L^2(\mathbb{R})} (\widehat{\mathbb{T}}_{p_2}, \widehat{\mathbb{T}}_{q_2})_{L^2(\mathbb{R})} \cdots (\widehat{\mathbb{T}}_{p_d}, \widehat{\mathbb{T}}_{q_d})_{L^2(\mathbb{R})} \big\} \\
&\quad + \big\{ (\widehat{\mathbb{T}}_{p_1}, \widehat{\mathbb{T}}_{q_1})_{L^2(\mathbb{R})} (\widehat{\mathbb{T}}'_{p_2}, \widehat{\mathbb{T}}'_{q_2})_{L^2(\mathbb{R})} \cdots (\widehat{\mathbb{T}}_{p_d}, \widehat{\mathbb{T}}_{q_d})_{L^2(\mathbb{R})} \big\} \\
&\quad + \cdots + \big\{ (\widehat{\mathbb{T}}_{p_1}, \widehat{\mathbb{T}}_{q_1})_{L^2(\mathbb{R})} \cdots (\widehat{\mathbb{T}}_{p_{d-1}}, \widehat{\mathbb{T}}_{q_{d-1}})_{L^2(\mathbb{R})} (\widehat{\mathbb{T}}'_{p_d}, \widehat{\mathbb{T}}'_{q_d})_{L^2(\mathbb{R})} \big\} \\
&= \lambda_{p_1} \delta_{p_1 q_1} \cdots \delta_{p_d q_d} + \lambda_{p_2} \delta_{p_1 q_1} \cdots \delta_{p_d q_d} + \cdots + \lambda_{p_d} \delta_{p_1 q_1} \cdots \delta_{p_d q_d} \\
&= (\lambda_{p_1} + \cdots + \lambda_{p_d}) \delta_{pq} = |\lambda_p|_1 \delta_{pq}.
\end{aligned}$$

This ends the proof. □

Remarkably, the use of the Fourier-like MCF can diagonalize the integral fractional Laplacian in the Dunford–Taylor formulation.

THEOREM 3.2. *Using the tensorial Fourier-like MCFs as basis functions, the solution of* (3.18)–(3.19) *can be uniquely expressed as*

$$(3.25) \qquad u_N(x) = \sum_{p \in \Upsilon_N} \frac{\hat{f}_p}{\gamma + |\lambda_p|_1^s} \widehat{\mathbb{T}}_p(x), \quad x \in \mathbb{R}^d,$$

where $\widehat{\mathbb{T}}_p, \lambda_p$ *are defined in* (3.20), *and*

$$(3.26) \qquad \hat{f}_p = (I_N^d f, \widehat{\mathbb{T}}_p)_{L^2(\mathbb{R}^d)}, \quad p \in \Upsilon_N.$$

Proof. Write

$$(3.27) \qquad u_N = \sum_{p \in \Upsilon_N} \hat{u}_p \widehat{\mathbb{T}}_p(x), \quad w_N = \sum_{p \in \Upsilon_N} \hat{w}_p \widehat{\mathbb{T}}_p(x),$$

where w_N is the unique solution of (3.19) associated with u_N. For clarity, we split the proof into the following steps.

(i) We first show that w_N can be uniquely determined by u_N via

$$(3.28) \qquad w_N = \sum_{p \in \Upsilon_N} \frac{\hat{u}_p}{1 + t^2 |\lambda_p|_1} \widehat{\mathbb{T}}_p(x).$$

Substituting (3.27) into (3.19), and taking $\psi = \widehat{\mathbb{T}}_q$ in (3.19), we arrive at

$$\sum_{p \in \Upsilon_N} \hat{w}_p \big\{ t^2 (\nabla\widehat{\mathbb{T}}_p, \nabla\widehat{\mathbb{T}}_q)_{L^2(\mathbb{R}^d)} + (\widehat{\mathbb{T}}_p, \widehat{\mathbb{T}}_q)_{L^2(\mathbb{R}^d)} \big\} = \sum_{p \in \Upsilon_N} \hat{u}_p (\widehat{\mathbb{T}}_p, \widehat{\mathbb{T}}_q)_{L^2(\mathbb{R}^d)} \quad \forall q \in \Upsilon_N.$$

By the orthogonality (3.23), we obtain

$$\sum_{p \in \Upsilon_N} \hat{w}_p \big\{ t^2 |\lambda_p|_1 + 1 \big\} \delta_{pq} = \sum_{p \in \Upsilon_N} \hat{u}_p \delta_{pq} \quad \forall q \in \Upsilon_N,$$

which implies (3.28), as

$$\hat{w}_p = \frac{\hat{u}_p}{1 + t^2 |\lambda_p|_1} \quad \forall p \in \Upsilon_N.$$

(ii) We next prove the integral identity

$$(3.29) \qquad \int_0^\infty \frac{t^{1-2s}\,|\lambda_p|_1^{1-s}}{1+t^2|\lambda_p|_1}\,\mathrm{d}t = \frac{\pi}{2\sin(\pi s)} = \frac{1}{C_s}.$$

Indeed, using a change of variable $y = t\sqrt{|\lambda_p|_1}$, we find readily that

$$\int_0^\infty \frac{t^{1-2s}\,|\lambda_p|_1^{1-s}}{1+t^2|\lambda_p|_1}\mathrm{d}t = \int_0^\infty \frac{y^{1-2s}}{1+y^2}\mathrm{d}y = \frac{\pi}{2\sin(\pi s)},$$

where we used the known formula (3.30) below with $\mu = 2 - 2s$ and $\nu = 2$. According to [25, pp. 325, 918, 905], we have for $\nu \ge \mu \ge 0$ and $\nu \ne 0$,

$$(3.30) \qquad \int_0^\infty \frac{x^{\mu-1}}{1+x^\nu}\mathrm{d}x = \frac{1}{\nu}\mathrm{B}\Big(\frac{\mu}{\nu}, 1 - \frac{\mu}{\nu}\Big) = \frac{1}{\nu}\Gamma\Big(\frac{\mu}{\nu}\Big)\Gamma\Big(1 - \frac{\mu}{\nu}\Big) = \frac{\pi}{\nu\sin(\pi\mu/\nu)},$$

where we used the properties of the Beta and Gamma functions

$$\mathrm{B}(x, y) = \frac{\Gamma(x)\Gamma(y)}{\Gamma(x+y)}, \quad \Gamma(1-x)\Gamma(x) = \frac{\pi}{\sin(\pi x)}.$$

(iii) Finally, we can derive (3.25) with the aid of (3.28)–(3.29). It is evident that by (3.27)–(3.28),

$$(3.31) \qquad u_N - w_N = t^2 \sum_{p \in \Upsilon_N} \frac{|\lambda_p|_1}{1+t^2|\lambda_p|_1}\,\hat{u}_p\widehat{\mathbb{T}}_p(x).$$

Thus, substituting (3.31) into (3.18) with $v_N = \widehat{\mathbb{T}}_q$, we obtain from (3.23) and (3.29) that

$$\mathcal{B}_N(u_N, \widehat{\mathbb{T}}_q)$$

$$= \sum_{p \in \Upsilon_N} \hat{u}_p\bigg\{C_s \int_0^\infty t^{1-2s}\int_{\mathbb{R}^d}\frac{|\lambda_p|_1}{1+t^2|\lambda_p|_1}\widehat{\mathbb{T}}_p(x)\widehat{\mathbb{T}}_q(x)\mathrm{d}x\,\mathrm{d}t + \gamma(\widehat{\mathbb{T}}_p, \widehat{\mathbb{T}}_q)_{L^2(\mathbb{R}^d)}\bigg\}$$

$$= \sum_{p \in \Upsilon_N} \hat{u}_p\bigg\{\delta_{pq}\,C_s \int_0^\infty \frac{t^{1-2s}\,|\lambda_p|_1}{1+t^2|\lambda_p|_1}\mathrm{d}t + \gamma\delta_{pq}\bigg\}$$

$$= \sum_{p \in \Upsilon_N} \hat{u}_p\big(|\lambda_p|_1^s + \gamma\big)\delta_{pq} = (I_N^d f, \widehat{\mathbb{T}}_q)_{L^2(\mathbb{R}^d)},$$

which implies

$$(3.32) \qquad \hat{u}_p = \frac{(I_N^d f, \widehat{\mathbb{T}}_p)_{L^2(\mathbb{R}^d)}}{\gamma + |\lambda_p|_1^s} \quad \forall p \in \Upsilon_N.$$

Thus, we obtain (3.25)–(3.26) immediately. □

Remark 3.1. It is crucial to use the Fourier-like MCFs as the basis functions for both u_N and w_N, so that we can take advantage of the biorthogonality and explicitly evaluate the integration in t. In other words, under the Fourier-like basis, the stiffness matrix of the linear system of (3.18)–(3.19) becomes a diagonal matrix of the form

$$(3.33) \qquad \widehat{S} := \big(\Sigma \otimes I \otimes \cdots \otimes I + I \otimes \Sigma \otimes I \otimes \cdots \otimes I + \cdots + I \otimes \cdots \otimes I \otimes \Sigma\big)^s,$$

where Σ is defined in (2.9) and $\otimes$ denotes the tensor product operator as before.

Remark 3.2. The precomputation of the Fourier-like MCF basis functions (in one dimension) by solving the eigenvalue problem (2.9) requires $O(N^3)$ operations by a direct solver, but $O(N^2)$ for a suitable iterative solver. The main cost of solving the system (3.32) is devoted to the evaluation of the right-hand side and u_N from the coefficients $\{\hat{u}_p\}$, which can be carried out by the FFT related to Chebyshev polynomials.

4. Error estimates and numerical examples. In this section, we derive some relevant MCF approximation results, which are useful for the error estimates of the proposed MCF–spectral-Galerkin scheme.

4.1. Approximation by MCFs. Consider d-dimensional L^2-orthogonal projection: $\pi_N^d : L^2(\mathbb{R}^d) \to \mathbb{V}_N^d$ such that

$$(4.1) \qquad \int_{\mathbb{R}^d} (\pi_N^d u - u)(x) v(x)\, \mathrm{d}x = 0 \quad \forall v \in \mathbb{V}_N^d.$$

We intend to estimate the projection error in the fractional Sobolev norm, i.e., $\|\pi_N^d u - u\|_{H^s(\mathbb{R}^d)}$. For this purpose, we introduce some notation and spaces of functions.

For notational convenience, the pairs of functions $(u, \breve{u})$ and $(U, \breve{U})$ associated with the mapping (2.4) have the relations

$$(4.2) \qquad u(x) = U(y(x)), \quad \breve{u}(x) = \frac{u(x)}{g(x)} = \frac{U(y)}{G(y)} = \breve{U}(y),$$

where as in (2.7), $g(x) = (1+x^2)^{-1/2} = \sqrt{1-y^2} = G(y)$. Define the differential operators

$$(4.3) \qquad \begin{aligned} D_{x_j} u &:= \partial_{x_j}\big\{(1+x_j^2)^{\frac{1}{2}} u\big\} \frac{\mathrm{d}x_j}{\mathrm{d}y_j} = a(x_j)\partial_{x_j}\big\{(1+x_j^2)^{\frac{1}{2}} u\big\} = \partial_{y_j} \breve{U}, \\ D_{x_j}^{k_j} u &= a(x_j)\partial_{x_j}\Big\{a(x_j)\partial_{x_j}\Big\{\cdots\Big\{a(x_j)\partial_{x_j}\big\{(1+x_j^2)^{\frac{1}{2}} u\big\}\Big\}\cdots\Big\}\Big\} = \partial_{y_j}^{k_j} \breve{U} \end{aligned}$$

for $k_j \geq 1, 1 \leq j \leq d$, where $a(x_j) = dx_j/dy_j = (1+x_j^2)^{\frac{3}{2}}$. Correspondingly, we define the d-dimensional Sobolev space

$$(4.4) \qquad B^m(\mathbb{R}^d) = \big\{u : D_x^k u \in L^2_{\varpi^{k+1}}(\mathbb{R}^d),\ 0 \leq |k|_1 \leq m\big\}, \quad m = 0,1,2,\ldots,$$

where the differential operator and the weight function are

$$(4.5) \qquad D_x^k u = D_{x_1}^{k_1} \cdots D_{x_d}^{k_d} u, \quad \varpi^k(x) = \prod_{j=1}^{d}(1+x_j^2)^{-k_j}.$$

It is equipped with the norm and seminorm

$$(4.6) \qquad \begin{aligned} \|u\|_{B^m(\mathbb{R}^d)} &= \Big(\sum_{0 \leq |k|_1 \leq m} \big\|D_x^k u\big\|_{L^2_{\varpi^{1+k}}(\mathbb{R}^d)}^2\Big)^{\frac{1}{2}}, \\ |u|_{B^m(\mathbb{R}^d)} &= \Big(\sum_{j=1}^{d} \big\|D_{x_j}^m u\big\|_{L^2_{\varpi^{1+me_j}}(\mathbb{R}^d)}^2\Big)^{\frac{1}{2}}, \end{aligned}$$

where $e_j = (0,\ldots,1,\ldots,0)$ is the jth unit vector in $\mathbb{R}^d$.

THEOREM 4.1. *If $u \in B^m(\mathbb{R}^d)$ with integer $m \geq 1$, then we have*

$$(4.7) \qquad \|\pi_N^d u - u\|_{H^s(\mathbb{R}^d)} \leq cN^{s-m}|u|_{B^m(\mathbb{R}^d)}, \quad 0 \leq s \leq 1,$$

where c is a positive constant independent of N and u.

Proof. In view of (3.6), it is necessary to estimate the projection errors in the L^2- and H^1-norms. According to [48, Thms. 3.1–3.2], we have

$$(4.8) \qquad \|\pi_N^d u - u\|_{L^2(\mathbb{R}^d)} \leq cN^{-m}|u|_{B^m(\mathbb{R}^d)}$$

and

$$(4.9) \qquad \|\nabla(\pi_N^d u - u)\|_{L^2(\mathbb{R}^d)} \leq cN^{1-m}|u|_{B^m(\mathbb{R}^d)}.$$

Using Lemma 3.1 and (4.8)–(4.9), we arrive at

$$\|\pi_N^d u - u\|_{H^s(\mathbb{R}^d)} \leq cN^{s-m}|u|_{B^m(\mathbb{R}^d)}, \quad s \in [0, 1].$$

This ends the proof. □

We now turn to the error estimate for the interpolation operator. Let $\{y_j, \rho_j\}_{j=0}^N$ be the Chebyshev–Gauss quadrature nodes and weights on $\Lambda = (-1, 1)$. Denote the mapped nodes and weights by

$$(4.10) \qquad x_j = \frac{y_j}{\sqrt{1 - y_j^2}}, \quad \omega_j = \frac{\rho_j}{1 + y_j^2}, \quad 0 \leq j \leq N.$$

Then by the exactness of the Chebyshev–Gauss quadrature, we have

$$(4.11) \quad \begin{aligned} \int_{\mathbb{R}} u(x)v(x)\,\mathrm{d}x &= \int_{\Lambda} U(y)V(y)(1-y^2)^{-\frac{3}{2}}\,\mathrm{d}y = \int_{\Lambda} \breve{U}(y)\breve{V}(y)(1-y^2)^{-\frac{1}{2}}\,\mathrm{d}y \\ &= \sum_{j=0}^N \breve{U}(y_j)\breve{V}(y_j)\rho_j \quad \forall \breve{U} \cdot \breve{V} \in \mathbb{P}_{2N+1}, \end{aligned}$$

which, together with (2.6), implies the exactness of the quadrature

$$(4.12) \qquad \int_{\mathbb{R}} u(x)v(x)\,\mathrm{d}x = \sum_{j=0}^N u(x_j)v(x_j)\omega_j \quad \forall u \cdot v \in \mathbb{V}_{2N+1}.$$

We now introduce the one-dimensional interpolation operator $I_N : C(\mathbb{R}) \to \mathbb{V}_N$ such that

$$(4.13) \qquad I_N u(x_j) = u(x_j), \quad 0 \leq j \leq N.$$

With a little abuse of notation, we define the d-dimensional grids by $x_j = (x_{j_1}, \ldots, x_{j_d})$, $j \in \Upsilon_N$, where $\{x_{j_k}\}_{k=1}^d$ are the mapped Chebyshev–Gauss nodes, and the index set Υ_N is given in (3.22) as before. We now consider the d-dimensional MCF interpolation: $C(\mathbb{R}^d) \to \mathbb{V}_N^d$,

$$(4.14) \qquad I_N^d u(x_j) = I_N^{(1)} \circ \cdots \circ I_N^{(d)} u(x_j), \quad j \in \Upsilon_N,$$

where $I_N^{(k)} = I_N, 1 \leq k \leq d$, is the interpolation along the x_k-direction.

In the error analysis, we also need the L^2-estimate of the d-dimensional MCF interpolation. For a better description of the error, we introduce a second seminorm of $B^m(\mathbb{R}^d)$ for $m \geq 1$ as follows:

$$(4.15) \qquad [[u]]_{B^m(\mathbb{R}^d)} := \left\{ |u|^2_{B^m(\mathbb{R}^d)} + \sum_{j=1}^d \sum_{k \neq j} \left\| D_{x_k}^{m-1} D_{x_j} u \right\|^2_{L^d_{\varpi^{1+(m-1)e_k+e_j}}(\mathbb{R}^d)} \right\}^{\frac{1}{2}},$$

where the weight function ϖ and $|u|_{B^m(\mathbb{R}^d)}$ are defined in (4.5) and (4.6) as before.

We have the following L^2-estimates of the interpolation.

THEOREM 4.2. *For $u \in B^m(\mathbb{R}^d)$ with the integer $m \geq 2$, we have*

$$(4.16) \qquad \|I_N^d u - u\|_{L^2(\mathbb{R}^d)} \leq cN^{-m}[[u]]_{B^m(\mathbb{R}^d)},$$

where c is a positive constant independent of N and u.

Proof. Let $I_N^C : C(\Lambda) \to \mathbb{P}_N$ be the Chebyshev–Gauss interpolation operator. According to [45, Lem. 3.6], we have that for any $v \in L^2_\omega(\Lambda)$ and $v' \in L^2_{\omega^{-1}}(\Lambda)$ with $\omega(y) = (1 - y^2)^{-\frac{1}{2}}$,

$$(4.17) \qquad \|I_N^C v\|_{L^2_\omega(\Lambda)} \leq c\big(\|v\|_{L^2_\omega(\Lambda)} + N^{-1}\|(1 - y^2)^{\frac{1}{2}} v'\|_{L^2_\omega(\Lambda)}\big),$$

where c is a positive constant independent of N and v. Moreover, by [45, Thm. 3.41], we have the one-dimensional Chebyshev–Gauss interpolation error estimates,

$$(4.18) \quad \|(I_N^C v - v)'\|_{L^2_{\omega^{-1}}(\Lambda)} + N\|I_N^C v - v\|_{L^2_\omega(\Lambda)} \leq cN^{1-m}\|(1 - y^2)^{\frac{m}{2}} v^{(m)}\|_{L^2_\omega(\Lambda)}.$$

In view of (2.4), we have

$$(4.19) \qquad \|I_N^d u - u\|_{L^2(\mathbb{R}^d)} = \big\|I_N^{C,d}(U/G) - (U/G)\big\|_{L^2_\omega(\Lambda^d)} = \big\|I_N^{C,d}\breve{U} - \breve{U}\big\|_{L^2_\omega(\Lambda^d)},$$

where $G(y) = \prod_{j=1}^d G(y_j)$ and $I_N^{C,d} := I_N^{C,(1)} \circ \cdots \circ I_N^{C,(d)}$ with $I_N^{C,(k)} = I_N^C$.

For clarity, we only prove the results with $d = 2$, as it is straightforward to extend the results to the case with $d \geq 3$. By virtue of the triangle inequality, (4.17) and (4.18), we obtain that for $m \geq 2$,

$$\|I_N^{C,2}\breve{U} - \breve{U}\|_{L^2_\omega(\Lambda^2)} \leq \|I_N^{C,(1)}\breve{U} - \breve{U}\|_{L^2_\omega(\Lambda^2)} + \big\|I_N^{C,(1)} \circ \big(I_N^{C,(2)}\breve{U} - \breve{U}\big)\big\|_{L^2_\omega(\Lambda^2)}$$

$$\leq cN^{-m}\|(1 - y_1^2)^{\frac{m}{2}} \partial_{y_1}^m \breve{U}\|_{L^2_\omega(\Lambda^2)} + c\Big\{\|I_N^{C,(2)}\breve{U} - \breve{U}\|_{L^2_\omega(\Lambda^2)}$$

$$(4.20) \qquad + N^{-1}\big\|(1 - y_1^2)^{\frac{1}{2}} \partial_{y_1}\big(I_N^{C,(2)}\breve{U} - \breve{U}\big)\big\|_{L^2_\omega(\Lambda^2)}\Big\}$$

$$\leq cN^{-m}\Big\{\big\|(1 - y_1^2)^{\frac{m}{2}} \partial_{y_1}^m \breve{U}\big\|_{L^2_\omega(\Lambda^2)} + \big\|(1 - y_2^2)^{\frac{m}{2}} \partial_{y_2}^m \breve{U}\big\|_{L^2_\omega(\Lambda^2)}$$

$$+ \big\|(1 - y_1^2)^{\frac{1}{2}}(1 - y_2^2)^{\frac{m-1}{2}} \partial_{y_1} \partial_{y_2}^{m-1} \breve{U}\big\|_{L^2_\omega(\Lambda^2)}\Big\}.$$

Note that in the above derivation, we can switch the order of $I_N^{C,(1)}$ and $I_N^{C,(2)}$, so we can add the term $\big\|(1 - y_1^2)^{\frac{m-1}{2}}(1 - y_2^2)^{\frac{1}{2}} \partial_{y_1}^{m-1} \partial_{y_2} \breve{U}\big\|_{L^2_\omega(\Lambda^2)}$ in the upper bound. Then, we derive from (4.2), (4.3), and (4.20) that for $m \geq 2$,

$$\|I_N^{C,2}\breve{U} - \breve{U}\|_{L^2_\omega(\Lambda^2)} \leq cN^{-m}\Big\{\big\|(1 + x_1^2)^{-\frac{m+1}{2}}(1 + x_2^2)^{-\frac{1}{2}} D_{x_1}^m u\big\|_{L^2(\mathbb{R}^2)}$$

$$+ \big\|(1 + x_1^2)^{-\frac{1}{2}}(1 + x_2^2)^{-\frac{m+1}{2}} D_{x_2}^m u\big\|_{L^2(\mathbb{R}^2)} + \big\|(1 + x_1^2)^{-1}(1 + x_2^2)^{-\frac{m}{2}} D_{x_1} D_{x_2}^{m-1} u\big\|_{L^2(\mathbb{R}^2)}$$

$$+ \big\|(1 + x_1^2)^{-\frac{m}{2}}(1 + x_2^2)^{-1} D_{x_1}^{m-1} D_{x_2} u\big\|_{L^2(\mathbb{R}^2)}\Big\} \leq cN^{-m}[[u]]_{B^m(\mathbb{R}^2)}.$$

It is straightforward to extend the above derivation to $d \geq 3$. This completes the proof. $\qquad \square$

To conduct error analysis for the proposed MCF scheme, we assume that the error for solving the elliptic problem (3.19) is negligible (or, equivalently, the quadrature errors in evaluating the fractional Laplacian in the scheme can be ignored), so formally, we have $w_N = (\mathbb{I} - t^2 \Delta)^{-1} u_N$. It is noteworthy that the analysis of such an error is feasible for the finite element approximation of the fractional Laplacian in a bounded domain based on the Dunford–Taylor formulation in a bounded domain, though the proof is lengthy and much involved (see [11]). However, the analysis is largely open in this situation, mainly because the spectrum estimate of the fractional Laplacian operator in $\mathbb{R}^d$ appears unavailable, as opposed to the bounded domain case (see [11]).

PROPOSITION 4.1. *Assume that the elliptic problem (3.19) in the scheme (3.18) can be solved exactly. Then we have the estimate for $u \in B^{m_1}(\mathbb{R}^d)$ with integer $m_1 \geq 1$, and $f \in B^{m_2}(\mathbb{R}^d)$ with integer $m_2 \geq 2$,*

$$(4.21) \qquad \|u - u_N\|_{H^s(\mathbb{R}^d)} \leq c N^{s-m_1} |u|_{B^{m_1}(\mathbb{R}^d)} + c N^{-m_2} [[f]]_{B^{m_2}(\mathbb{R}^d)}, \quad s \in (0, 1),$$

where c is a positive constant independent of u, f, and N.

Proof. Under this assumption, we find from Lemma 3.2 that the scheme (3.18) can be written as finding $u_N \in \mathbb{V}_N^d$ such that

$$\mathcal{B}(u_N, v_N) = (I_N^d f, v_N) \quad \forall v_N \in \mathbb{V}_N^d.$$

Then by (3.8) and (3.9), we infer from a standard argument that

$$\|u - u_N\|_{H^s(\mathbb{R}^d)} \leq c(\|\pi_N^d u - u\|_{H^s(\mathbb{R}^d)} + \|I_N^d f - f\|_{L^2(\mathbb{R}^d)}).$$

Thus, the estimate (4.21) follows from Theorems 4.1 and 4.2 immediately. $\qquad \square$

Remark 4.1. In what follows, we shall validate the above assumption through several numerical tests. Indeed, we shall observe that the errors of solving (3.19) are insignificant, and the order of the numerical errors agrees with the estimated order.

4.2. Useful analytic formulas. We first derive analytical formulas for the fractional Laplacian of some functions with typical exponential or algebraic decay, upon which we construct the exact solutions to test the accuracy of the proposed method, and to validate the assumption in Proposition 4.1. Moreover, we reveal that the fractional Laplacian has a very different property from the usual Laplacian. For example, the image of an exponential function decays algebraically (see Proposition 4.2 below), as opposed to the usual one.

We have the following exact formulas for the Gaussian function and rational function, whose derivations are sketched in Appendices A and B, respectively.

PROPOSITION 4.2. *For real $s > 0$ and integer $d \geq 1$, we have that*

$$(4.22) \qquad (-\Delta)^s \{e^{-|x|^2}\} = \frac{2^{2s} \Gamma(s + d/2)}{\Gamma(d/2)} \, {}_1F_1\Big(s + \frac{d}{2}; \frac{d}{2}; -|x|^2\Big).$$

Moreover for noninteger $s > 0$ and $|x| \to \infty$, we have the asymptotic behavior

$$(4.23) \qquad (-\Delta)^s \{e^{-|x|^2}\} = -\frac{2^{2s} \sin(\pi s)}{\pi} \frac{\Gamma(s + d/2)\Gamma(1 + s)}{|x|^{d+2s}} \{1 + O(|x|^{-2})\}.$$

PROPOSITION 4.3. *For real $s, r > 0$, and integer $d \geq 1$, we have*

$$(4.24) \quad (-\Delta)^s \left\{ \frac{1}{(1 + |x|^2)^r} \right\} = \frac{2^{2s} \Gamma(s + \gamma) \Gamma(s + d/2)}{\Gamma(\gamma) \Gamma(d/2)} {}_2F_1 \left(s + r, s + \frac{d}{2}; \frac{d}{2}; -|x|^2 \right).$$

Moreover for noninteger $s > 0$ and $|x| \to \infty$, we have the asymptotic properties for $r \neq d/2$,

$$(4.25) \quad (-\Delta)^s \left\{ \frac{1}{(1 + |x|^2)^r} \right\} \sim \frac{1}{(1 + |x|^2)^{s + \mu}}, \quad \mu = \min\{r, d/2\},$$

while for $r = d/2$,

$$(4.26) \quad (-\Delta)^s \left\{ \frac{1}{(1 + |x|^2)^r} \right\} \sim \frac{\ln(1 + |x|^2)}{(1 + |x|^2)^{s + d/2}}.$$

4.3. Numerical results. We apply the MCF–spectral-Galerkin method to solve the model problem (3.7) in various situations.

Example 4.1 (accuracy test). We first consider (3.7) with the following exact solutions:

$$(4.27) \quad u_e(x) = e^{-|x|^2}, \quad u_a(x) = (1 + |x|^2)^{-r}, \quad r > 0, \ x \in \mathbb{R}^d.$$

In view of (4.22) and (4.24), the source terms $f_e(x)$ and $f_a(x)$ are, respectively, given by

$$(4.28)$$
$$f_e(x) = \gamma e^{-|x|^2} + \frac{2^{2s} \Gamma(s + d/2)}{\Gamma(d/2)} {}_1F_1 \left(s + \frac{d}{2}; \frac{d}{2}; -|x|^2 \right),$$
$$f_a(x) = \gamma (1 + |x|^2)^{-r} + \frac{2^{2s} \Gamma(s + r) \Gamma(s + d/2)}{\Gamma(r) \Gamma(d/2)} {}_2F_1 \left(s + r, s + \frac{d}{2}; \frac{d}{2}; -|x|^2 \right).$$

Now, we intend to use the error estimates in Propositions 4.2 and 4.3 to analytically calculate the expected order of convergence by the MCF scheme, and then verify the convergence order numerically. For this purpose, we consider a generic function of algebraic decay as follows:

$$(4.29) \quad w(x) = \frac{1}{(1 + |x|^2)^\mu}, \quad x \in \mathbb{R}^d, \ \mu > 0.$$

Using (4.3) and (4.15), we obtain from direct calculation that

$$(4.30)$$
$$\begin{aligned} D_{x_j} w(x) &= (1 + x_j^2)^{\frac{3}{2}} \partial_{x_j} \left\{ (1 + x_j^2)^{\frac{1}{2}} w(x) \right\} \\ &= (1 + x_j^2)(1 + |x|^2)^{-\mu - 1}(-2\mu x_j(1 + x_j^2) \\ &\quad + x_j(1 + |x|^2)) \sim |x_j|^{-2\mu + 3} \prod_{l \neq j} |x_l|^{-2\mu} \end{aligned}$$

and, similarly,

$$D_{x_k} D_{x_j} w(x) \sim |x_k|^{-2\mu + 3} |x_j|^{-2\mu + 3} \prod_{l \neq j} |x_l|^{-2\mu},$$

$$D_{x_k}^2 D_{x_j} w(x) \sim |x_k|^{-2\mu + 5} |x_j|^{-2\mu + 3} \prod_{l \neq j, k} |x_l|^{-2\mu}.$$

By an induction argument, we can show

$$
(4.31) \quad
\begin{aligned}
D_{x_k}^{m-1} D_{x_j} w(x) &\sim |x_k|^{-2\mu+2m-1} |x_j|^{-2\mu+3} \prod_{l\neq j,k} |x_l|^{-2\mu}, \quad j \neq k, \\
D_{x_k}^m w(x) &\sim |x_k|^{-2\mu+2m+1} \prod_{l\neq k} |x_l|^{-2\mu}.
\end{aligned}
$$

Thus, for $j \neq k$, we have

$$
(4.32) \quad
\begin{aligned}
I_{kj}(x) &:= |D_{x_k}^{m-1} D_{x_j} w(x)|^2 \varpi^{1+(m-1)e_k+e_j}(x) \\
&\sim |x_k|^{-4\mu+2m-2} |x_j|^{-4\mu+4} \prod_{l\neq j,k} |x_l|^{-2\mu-2},
\end{aligned}
$$

and for $1 \leq k \leq d$,

$$
(4.33) \quad I_{kk}(x) := |D_{x_k}^m w(x)|^2 \varpi^{1+me_k}(x) \sim |x_k|^{-4\mu+2m} \prod_{l\neq k} |x_l|^{-2\mu-2}.
$$

Then by (4.6), (4.15), and (4.33), we find that if $m < 2\mu - \frac{1}{2}$, then

$$
(4.34) \quad
\begin{aligned}
|w|^2_{B^m(\mathbb{R}^d)} &= \sum_{k=1}^d \int_{\mathbb{R}^d} I_{kk}(x)\mathrm{d}x < \infty, \\
[[w]]^2_{B^m(\mathbb{R}^d)} &= |w|^2_{B^m(\mathbb{R}^d)} + \sum_{j=1}^d \sum_{k\neq j} \int_{\mathbb{R}^d} I_{kj}(x)\mathrm{d}x < \infty.
\end{aligned}
$$

For the exact solution $u_e(x) = e^{-|x|^2}$, we have from (4.23) and (4.28) that $f_e(x) \sim (1+|x|^2)^{-s-d/2}$. Therefore, in this case, the error is dominated by the MCF interpolation approximation of $f_e(x)$. Therefore, using (4.34) with $\mu = s + d/2$, we conclude from Proposition 4.2 that the expected convergence is $O(N^{-(2s+d)+1/2+\varepsilon})$ for small $\varepsilon > 0$. Remarkably, the numerical results in Figures 1(a), (c), (e) almost agree with the theoretical prediction (see the dashed reference lines). Indeed, it is very different from the usual Laplacian (see Proposition 4.2); we do not expect the exponential convergence, but algebraic decay of the errors.

We now turn to the second case with the exact solution $u_a(x) = (1+|x|^2)^{-r}$, where we take $r = 2.3$ in the numerical tests. As $r > d/2$, we derive from Proposition 4.3 that $f_a(x) \sim (1+|x|^2)^{-s-d/2}$. Then by (4.34) and Proposition 4.2, we have the convergence behavior

$$
\|u_a - u_N\|_{H^s(\mathbb{R}^d)} = O(N^{s-m_1}) + O(N^{-m_2}), \quad m_1 < 2r - \frac{1}{2}, \; m_2 < 2s + d - \frac{1}{2}.
$$

This implies the convergence order $O(N^{-\min\{2r-s,2s+d\}+\frac{1}{2}+\varepsilon})$. Indeed, we observe from Figures 1(b), (d), (f) a good agreement again. For example, for $d = 3$ and $r = 2.3$, we have the rate $O(N^{-3.1+\varepsilon})$ for $s = 0.3$, while the rate $O(N^{-3.4+\varepsilon})$ for $s = 0.7$. Interestingly, there is a preasymptotic range where one observes a sub-geometric convergence from Figures 1(d), (f) for $d = 2, 3$, but after the preasymptotic range, the convergence rates become algebraic as predicted. Such a phenomenon has been also observed for the Laguerre function approximation (cf. [45, p. 277]).
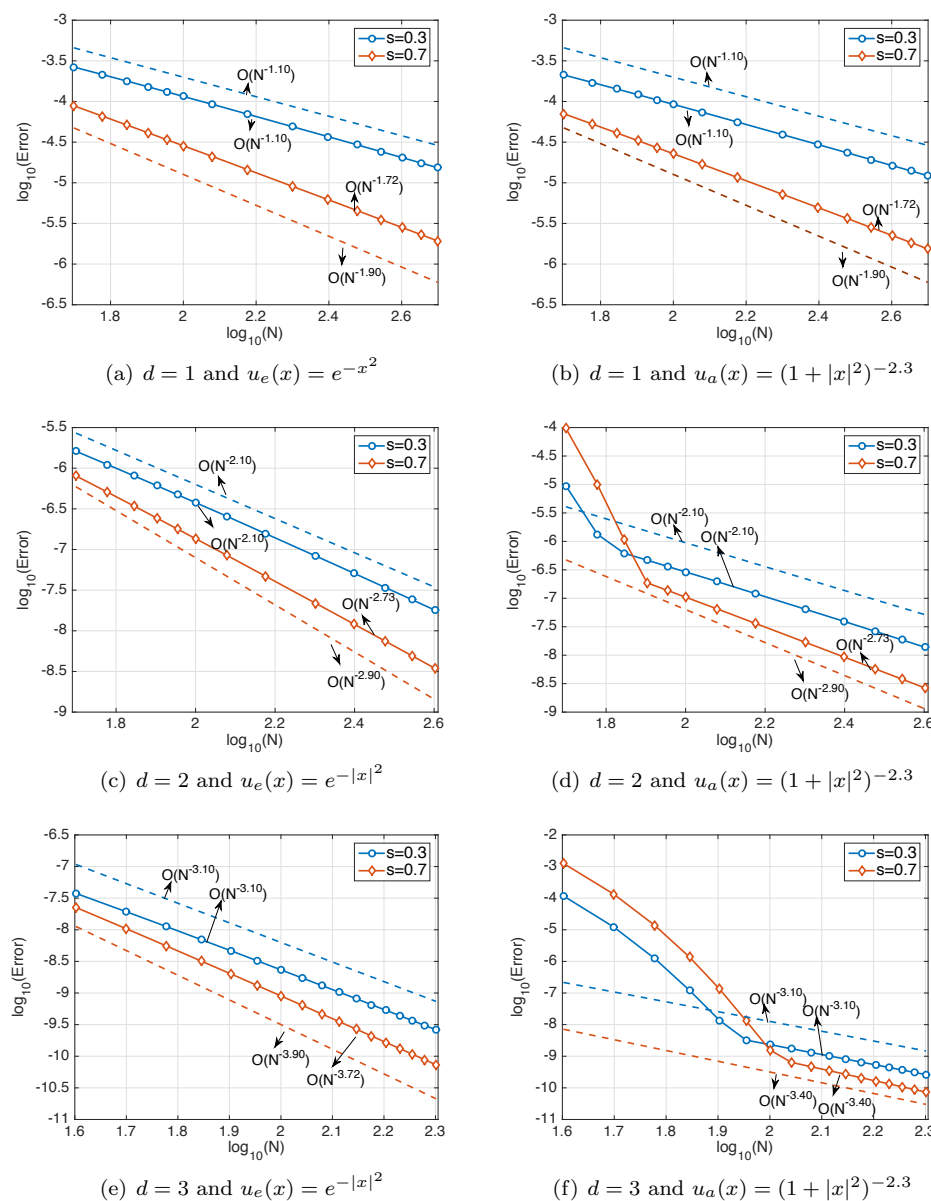
FIG. 1. *Decay of H^s-errors of the MCF scheme with $\gamma = 1$ and the scaling factor $\nu = 2.5$ for Example 4.1 with exact solutions in (4.27). Here $s = 0.3$, 0.7 and $r = 2.3$. The dashed reference lines are expected orders predicted by Proposition 4.1.*

Example 4.2 (effect of the scaling factor). It is known that, with a proper choice of the scaling parameter, the accuracy of the spectral method on the unbounded domain can be improved. In this example, we first show the influence of the scaling factor ν on the accuracy.

We plot in Figure 2(a) the maximum error in the log-log scale of our MCF algorithm with different scaling parameters ν. We observe from Figure 2(a) that for the
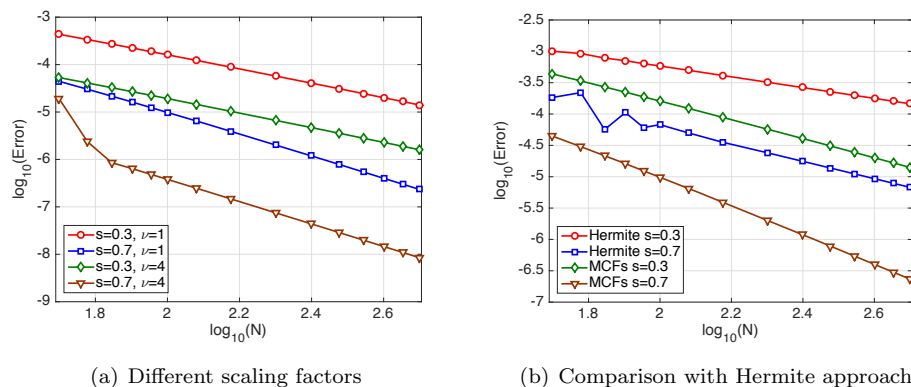
(a) Different scaling factors (b) Comparison with Hermite approach

FIG. 2. (a) *Maximum error for the exact solution $u(x) = (1 + x^2)^{-2.3}$ with different scaling factors ν, and $s = 0.3$, 0.7. (b) A comparison of the maximum error between our method and Hermite–Galerkin method* [37] *for the exact solution $u(x) = (1 + x^2)^{-2.3}$ with $s = 0.3$, 0.7, $\nu = 1$.*

same N and s, the approximations with $\nu = 4$ provide more accurate results than the approximations with $\nu = 1$; and for any fixed s, the two error curves are nearly parallel, which implies a proper scaling can improve the accuracy, but does not change the convergence order. In Figure 2(b), we compare the maximum errors of our algorithm using MCFs as basis functions with the Hermite spectral method in [37], for which we take $r = 2.3$. As we can see from Figure 2(b), the convergence rates of our approach are faster than that of the Hermite spectral method in [37].

Example 4.3 (accuracy for given source term $f(x)$). Here, we further compare our MCF method with the Hermite function approximation in [37], where the tests were provided for given source terms with unknown solutions.

We compute the reference "exact" solutions with large $N = 600$. In Figures 3(a)–(c), we compare the L^2-errors of our algorithm with the Hermite spectral method in [37] in one and two dimensions. It is noteworthy that the algorithm in [37] is computationally prohibitive for $d = 3$. In all cases, our approach outperforms the Hermite method in both accuracy and efficiency. We report in Figures 3(d)–(f) the maximum pointwise errors against various N's with $d = 2, 3$. The MCF method performs consistently well.

We also tabulate in Table 1 the L^2-errors and the convergence orders of two methods (see Tables 2 and 3 in [37] for the data on the Hermite method). Here, $f(x) = (1 + x)e^{-\frac{x^2}{2}}$, $s = 0.6$, 0.9, and $\nu = 2.5$. Observe that the MCF method possesses higher convergence rates.

Example 4.4 (multiterm fractional equations). Consider the three-dimensional multiterm fractional Laplacian equation

$$(4.35) \qquad \sum_{j=1}^{J} \rho_j (-\Delta)^{s_j} u(x) = f(x) \quad \text{in } \mathbb{R}^3, \quad u(x) \to 0 \quad \text{as } |x| \to \infty.$$

In Figure 4(a), we plot in log-log scale the maximum errors of (4.35) against various N, where we take $u(x) = (1 + |x|^2)^{-\frac{3\pi}{4}}$, $J = 4$, $s_1 = 0.77, s_2 = 0.33, s_3 = 0.21, s_4 = 0$, and $\rho_1 = 1, \rho_2 = 2, \rho_3 = \sqrt{2}, \rho_4 = 1$. In Figure 4(b), we plot in log-log scale the maximum errors of (4.35) against various N, where we take $f(x) = $
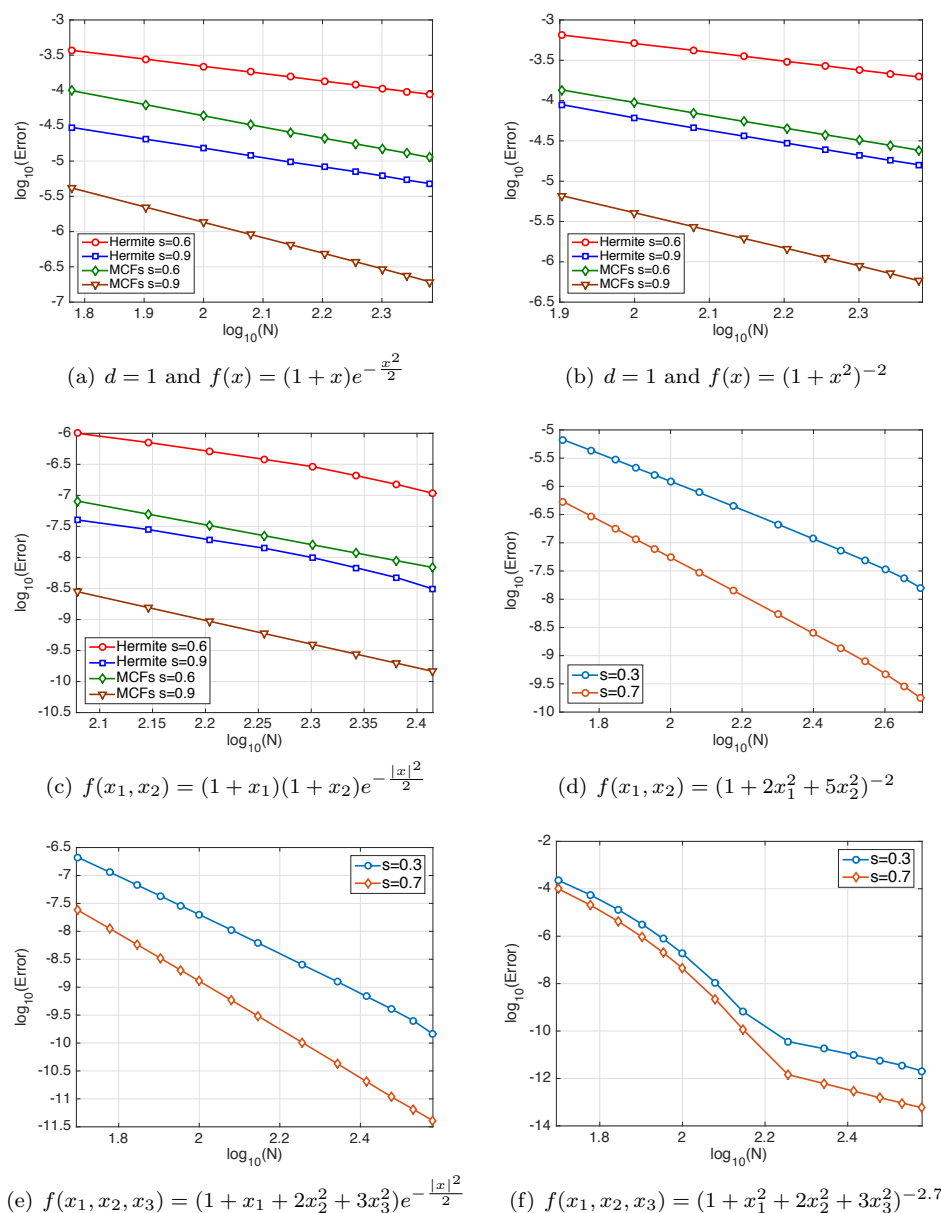
(a) $d = 1$ and $f(x) = (1+x)e^{-\frac{x^2}{2}}$

(b) $d = 1$ and $f(x) = (1+x^2)^{-2}$

(c) $f(x_1, x_2) = (1+x_1)(1+x_2)e^{-\frac{|x|^2}{2}}$

(d) $f(x_1, x_2) = (1 + 2x_1^2 + 5x_2^2)^{-2}$

(e) $f(x_1, x_2, x_3) = (1 + x_1 + 2x_2^2 + 3x_3^2)e^{-\frac{|x|^2}{2}}$

(f) $f(x_1, x_2, x_3) = (1 + x_1^2 + 2x_2^2 + 3x_3^2)^{-2.7}$

FIG. 3. (a)–(c) *A comparison of L^2-errors between our method and the Hermite–Galerkin method in* [37] *for different source functions $f(x)$.* (d)–(f) *The maximum errors for different source functions $f(x)$ with $d = 2, 3$. In the tests, we take $\gamma = 1, \nu = 2.5$.*

$(1 + x_1 + 2x_2^2 + 3x_3^2)e^{-\frac{|x|^2}{2}}$, $J = 4$, $s_1 = 0.76, s_2 = 0.41, s_3 = 0.23, s_4 = 0$, and $\rho_1 = 2, \rho_2 = 1, \rho_3 = 0.5, \rho_4 = 1$. We observe the algebraic decay of the errors, and the method is as accurate and efficient as the previous cases.

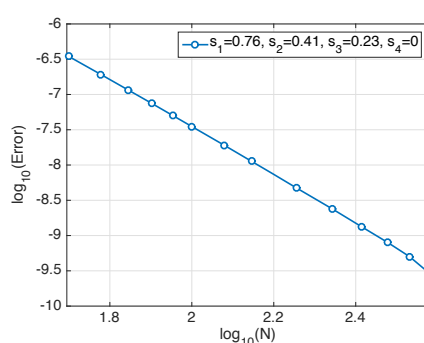**5. MCF approximation of nonlinear fractional Schrödinger equations.** In this section, we apply the fast algorithm to some nonlinear PDEs involving the

TABLE 1

A comparison of the L^2-error for $f(x) = (1+x)e^{-\frac{x^2}{2}}$.

	s = 0.6				s = 0.9			
N	Hermite [37]	Order	MCF	Order	Hermite [37]	Order	MCF	Order
80	2.77e-04		6.29e-05		2.06e-05		2.21e-06	
100	2.21e-04	1.01	4.38e-05	1.61	1.53e-05	1.32	1.35e-06	2.20
120	1.84e-04	1.02	3.26e-05	1.61	1.20e-05	1.33	9.10e-07	2.19
140	1.57e-04	1.03	2.56e-05	1.57	9.80e-06	1.33	6.51e-07	2.18
160	1.36e-04	1.03	2.08e-05	1.52	8.20e-06	1.34	4.86e-07	2.18
180	1.21e-04	1.04	1.75e-05	1.49	7.00e-06	1.34	3.75e-07	2.20
200	1.08e-04	1.04	1.49e-05	1.49	6.08e-06	1.34	2.96e-07	2.24
220	9.79e-05	1.05	1.29e-05	1.52	5.35e-06	1.34	2.38e-07	2.29
240	8.93e-05	1.06	1.12e-05	1.58	4.76e-06	1.35	1.94e-07	2.35
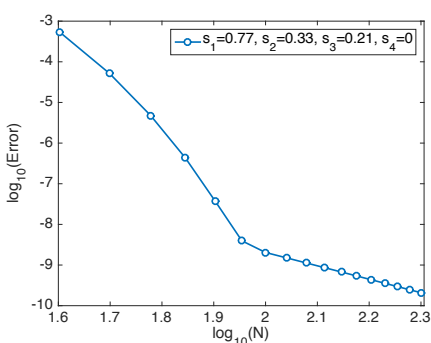
(a) $d = 3$ with given exact solution (b) $d = 3$ with given source term

FIG. 4. (a) *The maximum error for* (4.35) *with* $u(x) = (1+|x|^2)^{-\frac{3\pi}{4}}$ *and* $\nu = 2.5$. (b) *The maximum error for* (4.35) *with* $f(x) = (1+x_1+2x_2^2+3x_3^2)e^{-\frac{|x|^2}{2}}$ *and* $\nu = 2.5$.

fractional Laplacian. As an example, we consider the nonlinear fractional Schrödinger equation (fNLS) (cf. [33])

$$\text{(5.1)} \quad \begin{aligned} \mathrm{i}\psi_t &= \frac{1}{2}(-\Delta)^s\psi + \gamma|\psi|^2\psi, \quad x \in \mathbb{R}^d, \quad t \in (0, T], \\ \psi(x, 0) &= \psi_0(x), \quad x \in \mathbb{R}^d, \quad |\psi| \to 0 \text{ as } |x| \to \infty, \end{aligned}$$

where $\mathrm{i}^2 = -1$, $\psi(x, t)$ is a complex-valued wave function, the parameters γ is a real constant, and ψ_0 is given. It is noteworthy that the mass is conserved (cf. [7, 33]):

$$\text{(5.2)} \quad M(t) = \int_{\mathbb{R}^d} |\psi(x, t)|^2 \mathrm{d}x = M(0), \quad t > 0.$$

5.1. The scheme. We adopt the time-splitting technique, and start with rewriting the fNLS (5.1) as follows:

$$\text{(5.3)} \quad \mathrm{i}\psi_t = A\psi + B\psi,$$

where

$$A\psi = \gamma|\psi(x, t)|^2\psi(x, t), \quad B\psi = \frac{1}{2}(-\Delta)^s\psi(x, t).$$

The notion of time splitting is to solve the following two subproblems:

$$\text{(5.4)} \quad \mathrm{i}\frac{\partial\psi(x, t)}{\partial t} = A\psi(x, t) = \gamma|\psi(x, t)|^2\psi(x, t), \quad x \in \mathbb{R}^d,$$

and

$$(5.5) \qquad \mathrm{i}\frac{\partial \psi(x,t)}{\partial t} = B\psi(x,t) = \frac{1}{2}(-\Delta)^s \psi(x,t), \quad x \in \mathbb{R}^d.$$

The essence of the splitting method is to solve the two subproblems iteratively at each time step.

(i) We first consider the subproblem (5.4). Multiplying (5.4) by $\bar{\psi}(x,t)$, we find from the resulting equation that $|\psi(x,t)|$ is invariant in t (see, e.g., [7]). More precisely, for $t \geq t_s$ (t_s is any given time), (5.4) becomes

$$(5.6) \qquad \mathrm{i}\frac{\partial \psi(x,t)}{\partial t} = \gamma|\psi(x,t_s)|^2 \psi(x,t), \quad t \geq t_s, \quad x \in \mathbb{R}^d,$$

which can be integrated exactly, i.e.,

$$(5.7) \qquad \psi(x,t) = e^{-\mathrm{i}\gamma|\psi(x,t_s)|^2(t-t_s)}\psi(x,t_s), \quad t \geq t_s, \quad x \in \mathbb{R}^d.$$

(ii) We now turn to the subproblem (5.5). Remarkably, the Fourier-like basis can diagonalize the operator B so that $e^{-\mathrm{i}B\Delta t}\psi$ can be efficiently evaluated (which is crucial for the final scheme to be time reversible and time transverse invariant). More precisely, we seek $\psi_N(x,t) \in \mathbb{V}_N^d$ as an approximate solution to (5.5), such that

$$(5.8) \qquad \mathrm{i}\big(\partial_t \psi_N, v\big)_{L^2(\mathbb{R}^d)} = \big(B\psi_N, v\big)_{L^2(\mathbb{R}^d)} = \frac{1}{2}\big((-\Delta)^s \psi_N, v\big)_{L^2(\mathbb{R}^d)} \quad \forall v \in \mathbb{V}_N^d.$$

Using the Fourier-like MCF basis, we write

$$(5.9) \qquad \psi_N(x,t) = \sum_{k \in \Upsilon_N} \hat{\psi}_k(t)\widehat{\mathbb{T}}_k(x), \quad x \in \mathbb{R}^d.$$

Substituting it into (5.8), and taking the inner product with $\widehat{\mathbb{T}}_m(x)$, we deduce from (3.2) that

$$(5.10) \qquad \mathrm{i}\frac{\partial \hat{\psi}_m(t)}{\partial t} = \frac{1}{2}|\lambda_m|_1^s \hat{\psi}_m(t), \quad m \in \Upsilon_N.$$

Then, we derive from (5.10) that the solution for (5.8), i.e., the numerical solution of (5.5), is given by

$$(5.11) \qquad \psi_N(x,t) = e^{-\mathrm{i}B(t-t_s)}\psi_N(x,t_s) = \sum_{k \in \Upsilon_N} e^{-\frac{\mathrm{i}}{2}|\lambda_k|_1^s(t-t_s)}\hat{\psi}_k(t_s)\widehat{\mathbb{T}}_k(x), \quad t \geq t_s.$$

With the exact solution (5.7) and the approximate solution (5.11) for two subproblems (5.4) and (5.5), respectively, we now describe the implementation of the fourth-order time-splitting (TS4) method for solving (5.1). Let $\{x_p\}_{p \in \Upsilon_N}$ be tensorial grids as in (4.14), and $t_n = n\Delta t$ be the time-stepping grids. Let ψ_p^n be the approximation of $\psi(x_p, t_n)$, and denote by $\boldsymbol{\psi}^n$ the solution vector with components $\{\psi_p^n\}_{p \in \Upsilon_N}$. For notational convenience, we define the solution map related to (5.11):

$$(5.12) \qquad \mathcal{T}_N[\omega; \boldsymbol{\Psi}_p](x) = \sum_{k \in \Upsilon_N} e^{-\mathrm{i}\omega|\lambda_k|^s \Delta t} \hat{\Psi}_k \widehat{\mathbb{T}}_k(x),$$

where $\{\hat{\Psi}_k\}$ are the MCF expansion coefficients computed from the sampling of $\Psi \in \mathbb{V}_N^d$ on the grids $\{x_p\}$, and $\omega > 0$ is some weight.

TABLE 2
Time discretization errors for the TS4 method (5.13) *at* $T = 2$ *with* $N = 300$.

Δt	1/10	1/20	1/40	1/80	1/160	1/320
max-error	1.059e-02	1.092e-03	8.747e-05	5.782e-06	3.641e-07	2.301e-08
order	–	3.2	3.6	3.9	4.0	3.9
L^2-error	2.557e-03	2.235e-04	1.616e-05	1.084e-06	6.553e-08	4.435e-09
order	–	3.5	3.7	3.9	4.0	3.9

Following [7], we carry out the TS4 method for the fNLS (5.1), from time $t = t_n$ to $t = t_{n+1}$, as follows:

$$(5.13) \quad \begin{cases} \psi_p^{(1)} = e^{-2i\omega_1\gamma\Delta t|\psi_p^n|^2}\psi_p^n, & \psi_p^{(2)} = \mathcal{T}_N[\omega_2; \boldsymbol{\psi}^{(1)}](x_p), \\ \psi_p^{(3)} = e^{-2i\omega_3\gamma\Delta t\ |\psi_p^{(2)}|^2}\psi_p^{(2)}, & \psi_p^{(4)} = \mathcal{T}_N[\omega_4; \boldsymbol{\psi}^{(3)}](x_p), \\ \psi_p^{(5)} = e^{-2i\omega_3\gamma\Delta t|\psi_p^{(4)}|^2}\psi_p^{(4)}, & \psi_p^{(6)} = \mathcal{T}_N[\omega_2, \boldsymbol{\psi}^{(5)}](x_p), \\ \psi_p^{n+1} = e^{-2i\omega_1\gamma\Delta t\ |\phi_p^{(6)}|^2}\psi_p^{(6)} & \forall p \in \Upsilon_N, \end{cases}$$

where the weights are given by (cf. [56, 7])

$$(5.14) \quad \begin{aligned} &\omega_1 = 0.33780\ 17979\ 89914\ 40851, &&\omega_2 = 0.67560\ 35959\ 79828\ 81702, \\ &\omega_3 = -0.08780\ 17979\ 89914\ 40851, &&\omega_4 = -0.85120\ 71979\ 59657\ 63405. \end{aligned}$$

To show the stability of the fourth-order splitting method, we further define

$$(5.15) \quad \|\psi^n\|_N^2 = \sum_{j\in\Upsilon_N}|\psi_j^n|^2\omega_j := \sum_{j_1=0}^{N_1}\cdots\sum_{j_d=0}^{N_d}\psi(x_{j_1},\ldots,x_{j_d})\omega_{j_1}\cdots\omega_{j_d},$$

where $\psi_j^n = \psi^n(x_j)$, and $\{x_j, \omega_j\}_{j\in\Upsilon_N}$ are the corresponding tensorial nodes and weights as in (4.10). Following [7, Lemma 3.1], we can show the following property.

THEOREM 5.1. *The TS4 has the normalization conservation, i.e.,*

$$(5.16) \quad \|\psi^n\|_N^2 = \sum_{j\in\Upsilon_N}|\psi_j^n|^2\omega_j = \sum_{j\in\Upsilon_N}|\psi_0(x_j)|^2\omega_j = \|\psi_0\|_N^2, \quad n \geq 0.$$

5.2. Numerical results. In the computation, we take $d = 2$, and the initial condition to be

$$(5.17) \quad \psi_0(x_1, x_2) = \text{sech}(x_1)\text{sech}(x_2)\exp(i(x_1 + x_2)), \quad (x_1, x_2) \in \mathbb{R}^2.$$

In order to test the fourth-order accuracy in time of the TS4 method, we compute a numerical solution with focusing case $\gamma = -1$, $s = 0.7$, a very fine mesh, e.g., $N = 300$, and a very small time step $\Delta t = 0.0001$, as the exact solution ψ. Let $\psi^{\Delta t}$ be the numerical solution with $N = 300$ and time step size Δt. Table 2 lists the maximum error and L^2-error at $T = 2$ for different time step size Δt. The results in Table 2 demonstrate the fourth-order accuracy in time of the TS4 method (5.13).

In Figure 5, we plot the maximum errors and L^2-error versus space discretization N and time discretization Δt. They indicate that the numerical errors decay algebraically as N increases/or Δt decreases.

In Figures 6(a)–(b), we depict the modulus squared of the numerical solution with defocusing case ($\gamma = 1$) obtained by TS4. Here, we take $N = 200$, $T = 1, 2$, and
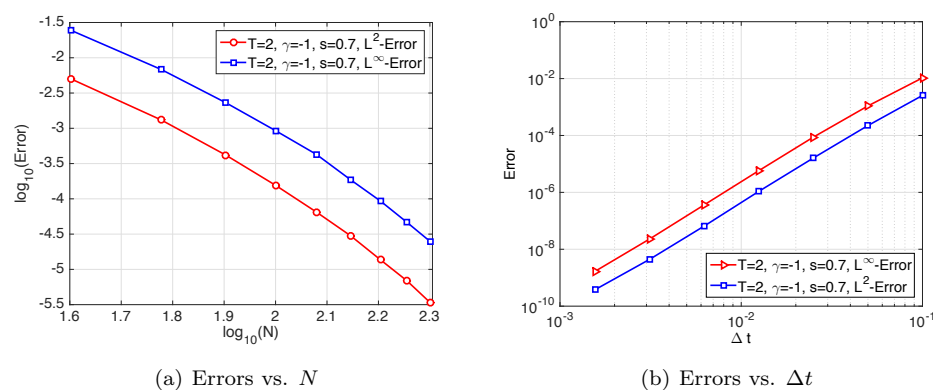
(a) Errors vs. N (b) Errors vs. Δt

FIG. 5. (a) *The numerical error of* (5.17) *with* $s = 0.7$, $\gamma = -1$, $T = 2$. (b) *The numerical error of* (5.17) *with* $s = 0.7$, $\gamma = -1$, $T = 2$.

(a) $T = 1$, $s = 0.3$ and $\gamma = 1$ (b) $T = 2$, $s = 0.3$ and $\gamma = 1$

(c) $T = 1$, $s = 0.3$ and $\gamma = -1$ (d) $T = 1$, $s = 0.7$ and $\gamma = -1$
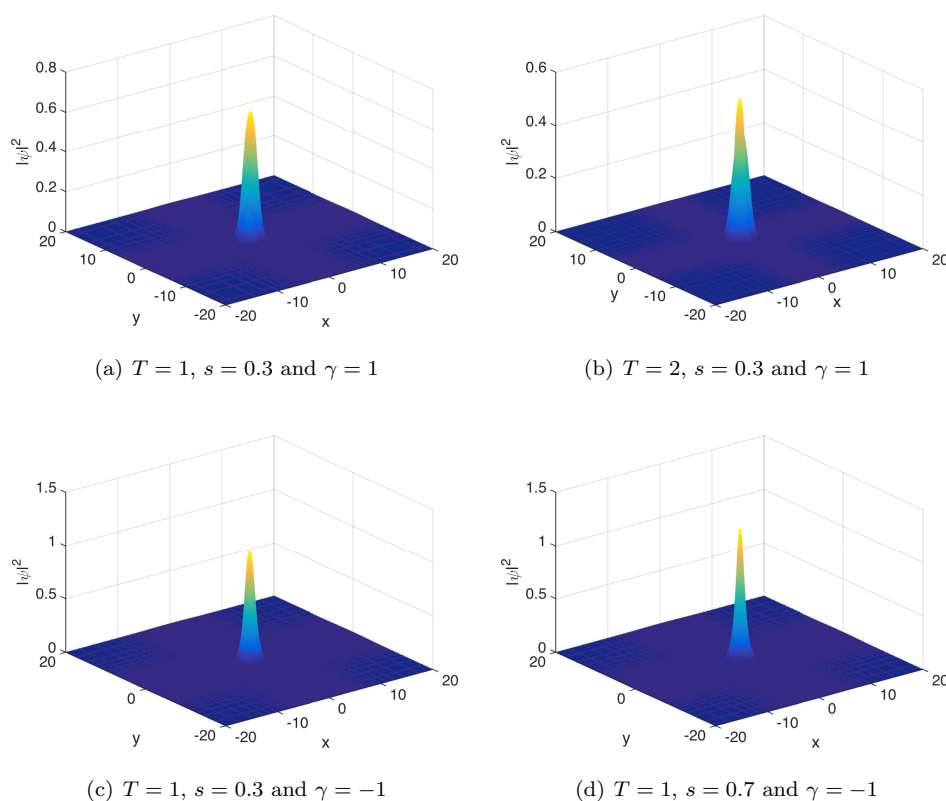
FIG. 6. *Profiles of the modulus square of the numerical solutions at different times and with different fractional orders.*

different values of fractional order $s = 0.3$. We observe that the solution diffused as expected. On the other hand, the blowup of the solution might happen for focusing case $\gamma = -1$ (cf. [33]). In Figures 6(c)–(d), we plot the profiles of the modulus square of the numerical solution at $T = 1$ with $N = 200$ and $s = 0.3, 0.7$. We can observe the expected blowup phenomenon.

5.3. Concluding remarks. We developed a fast spectral-Galerkin method using the mapped Chebyshev functions as the basis for PDEs involving the integral fractional Laplacian in $\mathbb{R}^d$. The fast solver is integrated with two critical components: (i) the Dunford–Taylor formulation for the fractional Laplacian; and (ii) Fourier-like biorthogonal MCFs as basis functions. The fast spectral algorithm could achieve a quasi-optimal computational cost. Different from the existing works on bounded domains (cf. [11, 12]), the integration in t is evaluated explicitly, and the fractional Laplacian can be fully diagonalized under (i) and (ii). Indeed, the existing approaches for the fractional Laplacian in unbounded domains are either too complicated or computationally prohibitive even for $d = 2$. However, the fast solver works for any dimension, and can be easily incorporated with, e.g., the hyperbolic cross and sparse grids (cf. [48]) when the dimension is high.

The proposed method can be extended to invert the operator $\mathbb{D}^s := (-\Delta + \theta\mathbb{I})^s$ with $s \in (0,1)$ and $\theta > 0$. In fact, one can verify readily that the Dunford–Taylor formulation in Lemma 3.2 takes the form

$$
\begin{aligned}
&\left(\mathbb{D}^{\frac{s}{2}}u, \mathbb{D}^{\frac{s}{2}}v\right)_{L^2(\mathbb{R}^d)} \\
&= C_s \int_0^\infty t^{1-2s} \int_{\mathbb{R}^d} \left((-\Delta + \theta\mathbb{I})\left(\mathbb{I} + t^2(-\Delta + \theta\mathbb{I})\right)^{-1}u\right)(x)\,v(x)\,\mathrm{d}x\,\mathrm{d}t.
\end{aligned}
$$

Then the fast algorithm in Theorem 3.2 can be extended to this case straightforwardly.

Appendix A. Proof of Proposition 4.2. The results with $d = 1$ were derived in [55], so it suffices to prove them for integer $d \geq 2$. Note that

$$
\begin{aligned}
\mathscr{F}\left\{e^{-|x|^2}\right\}(\xi) &= \frac{1}{(2\pi)^{d/2}} \int_{\mathbb{R}^d} e^{-|x|^2} e^{-\mathrm{i}x\cdot\xi} \mathrm{d}x \\
&= \frac{1}{(2\pi)^{d/2}} \int_{\mathbb{R}} e^{-x_1^2} e^{-\mathrm{i}x_1\xi_1} \mathrm{d}x_1 \cdots \int_{\mathbb{R}} e^{-x_d^2} e^{-\mathrm{i}x_d\xi_d} \mathrm{d}x_d = \frac{1}{2^{d/2}} e^{-\frac{|\xi|^2}{4}},
\end{aligned}
$$

where we used the identity (cf. [25, p. 339]):

$$
\int_{\mathbb{R}} e^{-x^2} e^{-\mathrm{i}x\xi} \mathrm{d}x = \sqrt{\pi} e^{-\frac{\xi^2}{4}}.
$$

Thus from the definition (1.1), we obtain

$$
\begin{aligned}
(A.1) \quad &(-\Delta)^s\left\{e^{-|x|^2}\right\}(x) \\
&= \mathscr{F}^{-1}\left\{|\xi|^{2s} \mathscr{F}\left\{e^{-|x|^2}\right\}(\xi)\right\} = \frac{1}{2^{d/2}(2\pi)^{d/2}} \int_{\mathbb{R}^d} |\xi|^{2s} e^{-\frac{|\xi|^2}{4}} e^{\mathrm{i}x\cdot\xi} \mathrm{d}\xi \\
&= \frac{2^d}{2^{d/2}(2\pi)^{d/2}} \int_{\mathbb{R}^d_+} |\xi|^{2s} e^{-\frac{|\xi|^2}{4}} \cos(x_1\xi_1)\cos(x_2\xi_2)\cdots\cos(x_d\xi_d)\mathrm{d}\xi.
\end{aligned}
$$

We proceed with the calculation by using the d-dimensional spherical coordinates:

$$
\begin{aligned}
(A.2) \quad &\xi_1 = r\cos\theta_1,\ \xi_2 = r\sin\theta_1\cos\theta_2,\cdots,\ \xi_{d-1} = r\sin\theta_1\cdots\sin\theta_{d-2}\cos\theta_{d-1}, \\
&\xi_d = r\sin\theta_1\cdots\sin\theta_{d-2}\sin\theta_{d-1},\quad r = |\xi|,
\end{aligned}
$$

so we can write

$$
(A.3) \quad (-\Delta)^s\left\{e^{-|x|^2}\right\}(x) = \frac{1}{\pi^{d/2}} \int_0^\infty r^{2s+d-1} e^{-\frac{r^2}{4}} \mathcal{I}(r;x)\mathrm{d}r,
$$

where

$$\mathcal{I}(r;x)$$

$$= \int_{[0,\frac{\pi}{2}]^{d-1}} \cos(rx_1\cos\theta_1)\cos(rx_2\sin\theta_1\cos\theta_2)\cdots\cos(rx_{d-1}\sin\theta_1\cdots\sin\theta_{d-2}\cos\theta_{d-1})$$

$$\cdot\cos(rx_d\sin\theta_1\cdots\sin\theta_{d-2}\sin\theta_{d-1})(\sin\theta_1)^{d-2}(\sin\theta_2)^{d-3}\cdots(\sin\theta_{d-2})\,\mathrm{d}\theta_1\mathrm{d}\theta_2\cdots\mathrm{d}\theta_{d-1}.$$

We first integrate $\mathcal{I}(r;x)$ with respect to θ_{d-1}. To do this, we recall the integral formula involving the Bessel functions (cf. [25, p. 732]): for real $\mu, \nu > -1$ and $a, b > 0$,

$$(A.4) \qquad \int_0^{\frac{\pi}{2}} J_\nu(a\sin\theta)J_\mu(b\cos\theta)\sin^{\nu+1}\theta\cos^{\mu+1}\theta\,\mathrm{d}\theta = \frac{a^\nu b^\mu J_{\nu+\mu+1}\left(\sqrt{a^2+b^2}\right)}{(a^2+b^2)^{(\nu+\mu+1)/2}}.$$

Then using the identity $\cos z = \sqrt{\pi z/2}J_{-1/2}(z)$ and (A.4) (with $a = rx_{d-1}\sin\theta_1$ $\cdots\sin\theta_{d-2}$, $b = rx_d\sin\theta_1\cdots\sin\theta_{d-2}$ and $\mu = \nu = -1/2$), we derive

$$\int_0^{\frac{\pi}{2}} \cos(rx_{d-1}\sin\theta_1\cdots\sin\theta_{d-2}\cos\theta_{d-1})\cos(rx_d\sin\theta_1\cdots\sin\theta_{d-2}\sin\theta_{d-1})\,\mathrm{d}\theta_{d-1}$$

$$= \frac{\pi}{2}J_0\big(r\sin\theta_1\cdots\sin\theta_{d-2}\sqrt{x_{d-1}^2+x_d^2}\,\big).$$

Substituting the above into $\mathcal{I}(r,x)$, and applying the same argument to $\theta_{d-2}, \theta_{d-3}, \ldots, \theta_1$ iteratively $d-2$ times, we obtain

$$(A.5) \qquad \mathcal{I}(r;x) = \left(\frac{\pi}{2}\right)^{\frac{d}{2}}(r|x|)^{1-\frac{d}{2}}J_{\frac{d}{2}-1}(r|x|).$$

We proceed with the integral identity (cf. [25, p. 713]): for real $\mu + \nu > -1$ and $p > 0$,

$$(A.6) \qquad \int_{\mathbb{R}^+} J_\mu(bt)e^{-p^2t^2}t^{\nu-1}\mathrm{d}t = \frac{b^\mu\Gamma((\mu+\nu)/2)}{2^{\mu+1}p^{\nu+\mu}\Gamma(\mu+1)}\,_1F_1\Big(\frac{\mu+\nu}{2};\mu+1;-\frac{b^2}{4p^2}\Big).$$

Then, substituting (A.5) into (A.3) and using (A.6) (with $\mu = d/2 - 1$ and $\nu = 2s + d/2 + 1$), we derive

$$(-\Delta)^s\big\{e^{-|x|^2}\big\} = \frac{|x|^{1-\frac{d}{2}}}{2^{d/2}}\int_0^\infty r^{2s+\frac{d}{2}}e^{-\frac{r^2}{4}}J_{\frac{d}{2}-1}(r|x|)\mathrm{d}r$$

$$= \frac{2^{2s}\Gamma(s+d/2)}{\Gamma(d/2)}\,_1F_1\Big(s+\frac{d}{2};\frac{d}{2};-|x|^2\Big).$$

This yields (4.22). The asymptotic behavior (4.23) follows from the property (cf. [8, p. 278]):

$$(A.7) \qquad \,_1F_1(a;b;z) = \frac{\Gamma(b)}{\Gamma(b-a)}(-z)^{-a}\big\{1 + O(|z|^{-1})\big\}.$$

Then (4.23) follows. This completes the proof.

Appendix B. Proof of Proposition 4.3. The identity with $d = 1$ can be found in [54], so we assume that $d \geq 2$. Using the d-spherical coordinate system in

(A.2), we obtain from (A.5) that

$$\mathscr{F}\Big\{\frac{1}{(1+|x|^2)^\gamma}\Big\}(\xi) = \frac{1}{(2\pi)^{d/2}}\int_{\mathbb{R}^d}\frac{e^{-\mathrm{i}x\cdot\xi}}{(1+|x|^2)^\gamma}\mathrm{d}x$$

$$= \frac{2^d}{(2\pi)^{d/2}}\int_{\mathbb{R}^d_+}\frac{\cos(x_1\xi_1)\cos(x_2\xi_2)\cdots\cos(x_d\xi_d)}{(1+|x|^2)^\gamma}\,\mathrm{d}x$$

$$= \Big(\frac{2}{\pi}\Big)^{\frac{d}{2}}\int_0^\infty\frac{r^{d-1}}{(1+r^2)^\gamma}\mathcal{I}(r;\xi)\,\mathrm{d}r = |\xi|^{1-\frac{d}{2}}\int_0^\infty\frac{r^{\frac{d}{2}}}{(1+r^2)^\gamma}J_{\frac{d}{2}-1}(r|\xi|)\mathrm{d}r.$$

Recall the integral formula (cf. [25, p. 686]): for $-1 < \nu < 2\mu + \frac{3}{2}$ and $a, b > 0$,

$$(B.1) \qquad \int_0^\infty\frac{x^{\nu+1}}{(x^2+a^2)^{\mu+1}}J_\nu(bx)\mathrm{d}x = \frac{a^{\nu-\mu}b^\mu}{2^\mu\Gamma(\mu+1)}K_{\nu-\mu}(ab),$$

where $K_\nu(x)$ is the modified Bessel function of the second kind. Note that $K_{-\nu}(x) = K_\nu(x)$. Then letting $\mu = \gamma - 1$ and $\nu = d/2 - 1$ in (B.1), we obtain

$$\mathscr{F}\Big\{\frac{1}{(1+|x|^2)^\gamma}\Big\}(\xi) = \frac{|\xi|^{\gamma-\frac{d}{2}}}{2^{\gamma-1}\Gamma(\gamma)}K_{\gamma-\frac{d}{2}}(|\xi|).$$

We also use the integral formula (cf. [25, p. 692]): for real $a > 0$, real b, and $\nu - \lambda + 1 > |\mu|$,

$$\int_0^\infty x^{-\lambda}K_\mu(ax)J_\nu(bx)\mathrm{d}x$$

$$(B.2) \qquad = \frac{b^\nu\Gamma\big((\nu-\lambda+\mu+1)/2\big)\Gamma\big((\nu-\lambda-\mu+1)/2\big)}{2^{\lambda+1}a^{\nu-\lambda+1}\Gamma(\nu+1)}$$

$$\times\; {}_2F_1\Big(\frac{\nu-\lambda+\mu+1}{2},\frac{\nu-\lambda-\mu+1}{2};\nu+1;-\frac{b^2}{a^2}\Big).$$

Once again, using the d-spherical coordinate system (A.2), (A.5), and (B.2) (with $\lambda = -2s - \gamma$, $\mu = \gamma - d/2$, and $\nu = d/2 - 1$), we have

$$(-\Delta)^s\Big\{\frac{1}{(1+|x|^2)^\gamma}\Big\} = \frac{1}{(2\pi)^{\frac{d}{2}}2^{\gamma-1}\Gamma(\gamma)}\int_{\mathbb{R}^d}e^{\mathrm{i}x\cdot\xi}|\xi|^{2s+\gamma-\frac{d}{2}}K_{\gamma-\frac{d}{2}}(|\xi|)\,\mathrm{d}\xi$$

$$= \frac{2^d}{(2\pi)^{\frac{d}{2}}2^{\gamma-1}\Gamma(\gamma)}\int_{\mathbb{R}^d_+}\cos(x_1\xi_1)\cos(x_2\xi_2)\cdots\cos(x_d\xi_d)|\xi|^{2s+\gamma-\frac{d}{2}}K_{\gamma-\frac{d}{2}}(|\xi|)\,\mathrm{d}\xi$$

$$= \frac{2^{\frac{d}{2}-\gamma+1}}{\pi^{\frac{d}{2}}\Gamma(\gamma)}\int_0^\infty r^{2s+\gamma+\frac{d}{2}-1}K_{\gamma-\frac{d}{2}}(r)\mathcal{I}(r,x)\,\mathrm{d}r$$

$$= \frac{2^{-\gamma+1}}{\Gamma(\gamma)}|x|^{1-\frac{d}{2}}\int_0^\infty r^{2s+\gamma}K_{\gamma-\frac{d}{2}}(r)J_{\frac{d}{2}-1}(r|x|)\mathrm{d}r$$

$$= \frac{2^{2s}\Gamma(s+\gamma)\Gamma(s+\frac{d}{2})}{\Gamma(\gamma)\Gamma(\frac{d}{2})}\,{}_2F_1\Big(s+\gamma, s+\frac{d}{2};\frac{d}{2};-|x|^2\Big).$$

This completes the derivation of (4.24).

According to [8, p. 76], the asymptotic behavior of the hypergeometric function for large $|x|$ (unless $a - b$ is an integer) is

$$(B.3) \qquad {}_2F_1(a,b;c;x) = \lambda_1|x|^{-a} + \lambda_2|x|^{-b} + O(|x|^{-a-1}) + O(|x|^{-b-1}),$$

where λ_1 and λ_2 are constants; if $a - b$ is an integer, z^{-a} or z^{-b} has to be multiplied by a factor $\ln(x)$. Then we have the asymptotic behavior of $(-\Delta)^s\big\{\frac{1}{(1+|x|^2)^\gamma}\big\}$ as $|x| \to \infty$ in (4.25)–(4.26).

REFERENCES

[1] G. ACOSTA, F. M. BERSETCHE, AND J. P. BORTHAGARAY, *A short FE implementation for a 2D homogeneous Dirichlet problem of a fractional Laplacian*, Comput. Math. Appl., 74 (2017), pp. 784–816.

[2] G. ACOSTA AND J. P. BORTHAGARAY, *A fractional Laplace equation: Regularity of solutions and finite element approximations*, SIAM J. Numer. Anal., 55 (2017), pp. 472–495.

[3] M. AGRANOVICH, *Sobolev Spaces, Their Generalizations and Elliptic Problems in Smooth and Lipschitz Domains*, Springer, Cham, Switzerland, 2015.

[4] M. AINSWORTH AND C. GLUSA, *Aspects of an adaptive finite element method for the fractional Laplacian: A priori and a posteriori error estimates, efficient implementation and multigrid solver*, Comput. Methods Appl. Mech. Engrg., 327 (2017), pp. 4–35.

[5] M. AINSWORTH AND C. GLUSA, *Hybrid finite element–spectral method for the fractional Laplacian: Approximation theory and efficient solver*, SIAM J. Sci. Comput., 40 (2018), pp. A2383–A2405.

[6] I. BABUŠKA, *Survey lectures on the mathematical foundations of the finite element method*, in The Mathematical Foundations of the Finite Element Method with Applicaions to Partial Differential Equations, Academic Press, New York, 1972, pp. 3–359.

[7] W. BAO AND J. SHEN, *A fourth-order time-splitting Laguerre–Hermite pseudospectral method for Bose–Einstein condensates*, SIAM J. Sci. Comput., 26 (2005), pp. 2010–2028.

[8] H. BATEMAN, *Higher Transcendental Functions*, Volumes I–III, McGraw-Hill, New York, 1953.

[9] D. A. BENSON, S. W. WHEATCRAFT, AND M. M. MEERSCHAERT, *Application of a fractional advection-dispersion equation*, Water Res. Res., 36 (2000), pp. 1403–1412.

[10] A. BONITO, J. P. BORTHAGARAY, R. H. NOCHETTO, E. OTÁROLA, AND A. J. SALGADO, *Numerical methods for fractional diffusion*, Comput. Vis. Sci., 19 (2018), pp. 19–46.

[11] A. BONITO, W. LEI, AND J. E. PASCIAK, *Numerical approximation of the integral fractional Laplacian*, Numer. Math., 142 (2019), pp. 235–278.

[12] A. BONITO, W. LEI, AND J. E. PASCIAK, *On sinc quadrature approximations of fractional powers of regularly accretive operators*, J. Numer. Math., 27 (2019), pp. 57–68.

[13] D. BROCKMANN, L. HUFNAGEL, AND T. GEISEL, *The scaling laws of human travel*, Nature, 439 (2006), pp. 462–465.

[14] L. CAFFARELLI AND L. SILVESTRE, *An extension problem related to the fractional Laplacian*, Comm. Partial Differential Equations, 32 (2007), pp. 1245–1260.

[15] B. CARMICHAEL, H. BABAHOSSEINI, S. MAHMOODI, AND M. AGAH, *The fractional viscoelastic response of human breast tissue cells*, Phys. Biol., 12 (2015), 046001.

[16] L. CHEN, Z. MAO, AND H. LI, *Jacobi-Galerkin Spectral Method for Eigenvalue Problems of Riesz Fractional Differential Equations*, preprint, arXiv:1803.03556, 2018.

[17] S. CHEN, J. SHEN, AND L.-L. WANG, *Laguerre functions and their applications to tempered fractional differential equations on infinite intervals*, J. Sci. Comput., 74 (2018), pp. 1286–1313.

[18] J. H. CUSHMAN AND T. GINN, *Nonlocal dispersion in media with continuously evolving scales of heterogeneity*, Transp. Porous Media, 13 (1993), pp. 123–138.

[19] M. D'ELIA, Q. DU, C. GLUSA, M. GUNZBURGER, X. TIAN, AND Z. ZHOU, *Numerical methods for nonlocal and fractional models*, Acta Numer., to appear.

[20] W. DENG, *Finite element method for the space and time fractional Fokker–Planck equation*, SIAM J. Numer. Anal., 47 (2008), pp. 204–226.

[21] W. DENG, B. LI, Z. QIAN, AND H. WANG, *Time discretization of a tempered fractional Feynman–Kac equation with measure data*, SIAM J. Numer. Anal., 56 (2018), pp. 3249–3275.

[22] Q. DU, *Nonlocal Modeling, Analysis, and Computation*, CBMS-NSF Regional Conf. Ser. in Appl. Math. 94, SIAM, Philadelphia, 2019.

[23] S. DUO AND Y. ZHANG, *Computing the ground and first excited states of the fractional Schrödinger equation in an infinite potential well*, Commun. Comput. Phys., 18 (2015), pp. 321–350.

[24] S. DUO AND Y. ZHANG, *Accurate numerical methods for two and three dimensional integral fractional Laplacian with applications*, Comput. Methods Appl. Mech. Engrg., 355 (2019), pp. 639–662.

[25] I. S. Gradshteyn and I. M. Ryzhik, *Table of Integrals, Series, and Products*, 8th ed., Elsevier/Academic Press, Amsterdam, 2015.

[26] B. Guo and Z. Wang, *Modified Chebyshev rational spectral method for the whole line*, in Proceedings of the Fourth International Conference on Dynamical Systems and Differential Equations, American Mathematical Society, Providence, RI, 2002, pp. 365–374.

[27] X. Guo, Y. Li, and H. Wang, *A high order finite difference method for tempered fractional diffusion equations with applications to the CGMY model*, SIAM J. Sci. Comput., 40 (2018), pp. A3322–A3343.

[28] Y. Hatano and N. Hatano, *Dispersive transport of ions in column experiments: An explanation of long-tailed profiles*, Water Res. Res., 34 (1998), pp. 1027–1033.

[29] D. Hou and C. Xu, *A fractional spectral method with applications to some singular problems*, Adv. Comput. Math., 43 (2017), pp. 911–944.

[30] Y. Huang and A. Oberman, *Numerical methods for the fractional Laplacian: A finite difference-quadrature approach*, SIAM J. Numer. Anal., 52 (2014), pp. 3056–3084.

[31] B. Jin, R. Lazarov, and Z. Zhou, *Error estimates for a semidiscrete finite element method for fractional order parabolic equations*, SIAM J. Numer. Anal., 51 (2013), pp. 445–466.

[32] B. Jin, B. Li, and Z. Zhou, *Numerical analysis of nonlinear subdiffusion equations*, SIAM J. Numer. Anal., 56 (2018), pp. 1–23.

[33] C. Klein, C. Sparber, and P. Markowich, *Numerical study of fractional nonlinear Schrödinger equations*, Proc. A, 470 (2014), 20140364.

[34] A. Lischke, G. Pang, M. Gulian, F. Song, C. Glusa, X. Zheng, Z. Mao, W. Cai, M. Meerschaert, M. Ainsworth, and G. Karniadakis, *What is the fractional Laplacian? A comparative review with new results*, J. Comput. Phys., 404 (2020), 109009.

[35] H. Ma, W. Sun, and T. Tang, *Hermite spectral methods with a time-dependent scaling for parabolic equations in unbounded domains*, SIAM J. Numer. Anal., 43 (2005), pp. 58–75.

[36] Z. Mao, S. Chen, and J. Shen, *Efficient and accurate spectral method using generalized Jacobi functions for solving Riesz fractional differential equations*, Appl. Numer. Math., 106 (2016), pp. 165–181.

[37] Z. Mao and J. Shen, *Hermite spectral methods for fractional PDEs in unbounded domains*, SIAM J. Sci. Comput., 39 (2017), pp. A1928–A1950.

[38] B. McCay and M. N. L. Narasimhan, *Theory of nonlocal electromagnetic fluids*, Arch. Mech., 33 (1981), pp. 365–384.

[39] R. Metzler and J. Klafter, *The random walk's guide to anomalous diffusion: A fractional dynamics approach*, Phys. Rep., 339 (2000), pp. 1–77.

[40] R. Metzler and J. Klafter, *The restaurant at the end of the random walk: Recent developments in the description of anomalous transport by fractional dynamics*, J. Phys. A, 37 (2004), pp. 161–208.

[41] E. W. Montroll and G. H. Weiss, *Random walks on lattices.* II, J. Math. Phys., 6 (1965), pp. 167–181.

[42] E. D. Nezza, G. Palatucci, and E. Valdinoci, *Hitchhiker's guide to the fractional Sobolev spaces*, Bull. Sci. Math., 136 (2012), pp. 521–573.

[43] R. H. Nochetto, E. Otárola, and A. J. Salgado, *A PDE approach to fractional diffusion in general domains: A priori error analysis*, Found. Comput. Math., 15 (2014), pp. 733–791.

[44] R. H. Nochetto, E. Otárola, and A. J. Salgado, *A PDE approach to space-time fractional parabolic problems*, SIAM J. Numer. Anal., 54 (2016), pp. 848–873.

[45] J. Shen, T. Tang, and L.-L. Wang, *Spectral Methods: Algorithms, Analysis and Applications*, Springer Ser. Comput. Math. 41, Springer, Berlin, 2011.

[46] J. Shen and L.-L. Wang, *Error analysis for mapped Legendre spectral and pseudospectral methods*, SIAM J. Numer. Anal., 42 (2004), pp. 326–349.

[47] J. Shen and L.-L. Wang, *Some recent advances on spectral methods for unbounded domains*, Commun. Comput. Phys., 5 (2009), pp. 195–241.

[48] J. Shen, L.-L. Wang, and H. Yu, *Approximations by orthonormal mapped Chebyshev functions for higher-dimensional problems in unbounded domains*, J. Comput. Appl. Math., 265 (2014), pp. 264–275.

[49] M. Shlesinger, B. West, and J. Klafter, *Lévy dynamics of enhanced diffusion: Application to turbulence*, Phys. Rev. Lett., 58 (1987), pp. 1100–1103.

[50] S. A. Silling, *Reformulation of elasticity theory for discontinuities and long-range forces*, J. Mech. Phys. Solids, 48 (2000), pp. 175–209.

[51] D. W. Sims et al., *Scaling laws of marine predator search behaviour*, Nature, 451 (2008), pp. 1098–1102.

[52] G. Szegö, *Orthogonal Polynomials*, Vol. 23, American Mathematical Society, Providence, RI, 1939.

[53] T. TANG, *The Hermite spectral method for Gaussian-type functions*, SIAM J. Sci. Comput., 14 (1993), pp. 594–606.

[54] T. TANG, L.-L. WANG, H. YUAN, AND T. ZHOU, *Rational spectral methods for PDEs involving fractional Laplacian in unbounded domains*, SIAM J. Sci. Comput., 42 (2020), pp. A585–A611.

[55] T. TANG, H. YUAN, AND T. ZHOU, *Hermite spectral collocation methods for fractional PDEs in unbounded domains*, Commun. Comput. Phys., 24 (2018), pp. 1143–1168.

[56] H. YOSHIDA, *Construction of higher order symplectic integrators*, Phys. Lett. A, 150 (1990), pp. 262–268.

[57] Z. ZHANG, W. DENG, AND G. E. KARNIADAKIS, *A Riesz basis Galerkin method for the tempered fractional Laplacian*, SIAM J. Numer. Anal., 56 (2018), pp. 3010–3039.